Advances in Neurology, Vol. 44, edited by
A. V. Delgado-Escueta, A. A. Ward, Jr.,
D. M. Woodbury, and R. J. Porter.
Raven Press, New York © 1986.

11

Membrane Currents Underlying Bursting Pacemaker Activity and Spike Frequency Adaptation in Invertebrates

*Darrell V. Lewis, **John R. Huguenard, †William W. Anderson, and †Wilkie A. Wilson

*Departments of *Pediatrics, Medicine, and †Pharmacology, Duke University, Durham, North Carolina, and Department of **Neurology, Stanford University Medical Center, Stanford, California 94305*

SUMMARY Invertebrate systems have proved to be quite useful for the development of an understanding of some processes in the central nervous system (CNS). An understanding of the basic mechanisms of epilepsy will result from understanding not only how populations of neurons interact but also how the physiological processes in individual neurons are altered in epileptogenesis. Because invertebrate neurons have been so accessible to experimentation, it has been possible to explore in detail the basic mechanisms controlling neuronal excitability using these cells and to make some useful predictions about electrophysiological mechanisms that may be present in central neurons.

This chapter deals with two electrophysiological processes that have been observed in invertebrate neurons and that may have some relevance to understanding the basic mechanisms of epilepsy. We review first the past and current studies of invertebrate burst firing neurons. It appears that the electrophysiological mechanisms producing burst firing may be present in CNS neurons participating in epileptogenesis. With caution, the information gleaned from invertebrate studies may be applicable to higher systems.

The second process we consider is the phenomenon of spike frequency adaptation seen in invertebrates. Spike frequency adaptation is the process by which the firing rate of the neuron declines despite the maintenance of a constant stimulus. This process is not so thoroughly studied as burst firing, but it appears to represent a cellular mechanism designed to suppress prolonged periods of repetitive firing. Clearly, the suppression of such a process would produce excessive neuronal excitability, while its enhancement might have some anticonvulsant effects. The extreme sensitivity of spike frequency adaptation to barbiturates suggests such a possibility.

These two electrophysiological processes are interesting in themselves and also because they may underlie the genesis or control of seizures. However, the greater significance is that, to understand the basic mechanisms of epilepsy, we may be well advised to examine neuronal processes in systems not considered to have seizure susceptibility.

The rhythmic, repetitive bursts of action potentials generated by certain autoactive invertebrate neurons have fascinated many neurobiologists. These bursting pacemaker neurons (BPNs) are large, identifiable cells which generate, independent of any synaptic input, rhythmically recurring bursts of action potentials. After each burst, the BPN abruptly hyperpolarizes. Subsequently, the cell slowly depolarizes until spike threshold is reached many seconds later and the next burst begins and the cycle is repeated. Numerous experiments have confirmed that the slow membrane currents underlying the bursting rhythm are not synaptic but are endogenous to the BPN membrane (6,24,92). The marked influx of calcium with each burst is a crucial modulator of these slow currents (Fig. 1). In addition, neurotransmitters and peptides can modulate bursting pacemaker activity (BPA) by altering these endogenous conductances.

The BPA of invertebrate neurons resembles the bursting activity encountered in neurons in experimental vertebrate models of epilepsy. This resemblance has suggested that understanding the basic mechanisms of invertebrate BPA might give some insight into mechanisms of bursting in epilepsy. Indeed, several ionic conductances underlying BPA initially described in studies of invertebrates have been paralleled by later discoveries of similar currents involved in bursting in hippocampal pyramidal cells. Nevertheless, the superficial similarity between BPA and epileptiform bursting should not be assumed to imply identical underlying mechanisms.

This review will concentrate on the evolution of our concepts of BPA, which, as will become apparent, are still developing. In spite of the relative ease of experimenting with these large, hardy, easily identifiable neurons and the intensive efforts expended upon them in the last 10 to 15 years, new insights into the nature and control of the slow currents governing bursting are still occurring. Direct comparisons with the literature of epilepsy will not be attempted, but it is hoped that reading this account of the efforts to understand bursting will be of some indirect, philosophical, and perhaps scientific, value to the epileptologist who is grappling with the even more complex problem of epileptiform bursting.

OVERVIEW OF BURSTING PACEMAKER ACTIVITY

A brief description of the currents regulating BPA will be helpful in understanding the detailed review of their mechanisms to follow. Present models of bursting (12,20,21,40,47,75,83,92) attribute to slow potential oscillations to two slow current systems. These currents are smaller and slower in their activation and inactivation kinetics than the classical action potential currents. The slow inward current (SIC) is a calcium and/or sodium current, activated by depolarization. It has very gradual and incomplete inactivation; thus, it is frequently referred to as a persistent inward current or steady state inward current. The slow outward current (SOC) is a hyperpolarizing current that is activated by increased intracellular calcium activity, $[Ca]_i$, and has a very slow time course (many seconds) often appearing to reflect the time course of changes in $[Ca]_i$. As will be discussed, the exact

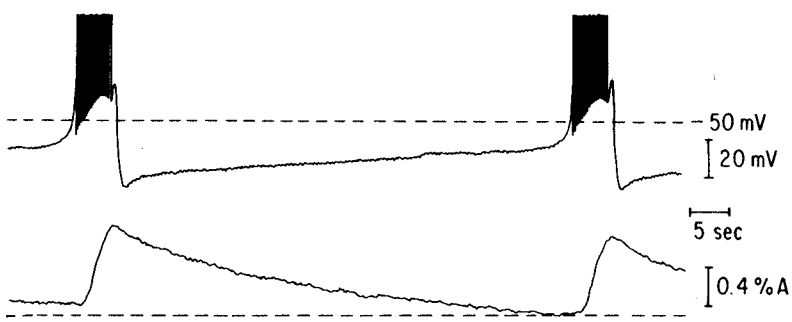

FIG. 1. Bursting pacemaker activity and the corresponding changes of intracellular calcium. **Upper trace:** voltage-measured at soma during spontaneous bursting. In this example, each burst contains about 50 spikes. **Lower trace:** absorbance of intracellular Arsenazo III measured at the soma (660–700 nM). As intracellular calcium activity, $[Ca]_i$, increases, the absorbance increases. Thus, during the burst, there is a rise of $[Ca]_i$ indicated by the upswing of the absorbance trace. During the interburst interval $[Ca]_i$ slowly declines. (D. V. Lewis, unpublished data, July 1981.)

ionic basis of the SOC and SIC are at present debated.

The SIC and SOC can be demonstrated using voltage clamp commands in a BPN. In Fig. 2A, the cell is held at −50 mV, and then is given depolarizing commands to several membrane voltages at which the SIC is activated. The commands are 10 sec in duration because of the slow kinetics of the currents being measured. When the current values 1.5 sec after the beginning of the commands are plotted, the current–voltage (I/V) curve shows a prominent region of negative slope (Fig. 2B), in this instance above −50 mV. This negative slope resistance (NSR) region of the I/V curve is caused by the voltage-dependent activation of the SIC. The NSR region clearly implies an unstable situation. If the cell were to come to rest at any voltage in this region, the inward membrane current would depolarize the cell further, activating more SIC, causing more depolarization, etc.

The SOC also can be seen in Fig. 2A. Note the outward tail current following the 10-sec depolarizations. This tail, the SOC, becomes larger with the larger depolarizations and decays with a slow, many seconds long, time course (57). The partial relaxation of the SIC seen during the commands, which also is more prominent with the greater depolarizations, may represent the same process that gives rise to the SOC tails. Evidence yet to be discussed in detail indicates that the SOC is caused by calcium that enters the cell during depolarization (Fig. 2C).

These illustrations reflect current concepts of the roles of the SIC and SOC in bursting. Beginning at the most hyperpolarized point in the bursting cycle, the SOC is maximum as a result of the massive increase of $[Ca]_i$ during the spikes of the preceding burst (Fig. 1). As the $[Ca]_i$ gradually declines as a result of sequestration and extrusion, the SOC also decreases, allowing the cell to begin to depolarize slightly. The depolarization ultimately begins to activate the regenerative SIC, which drives the depolarization more rapidly. Soon spike threshold is reached and the burst begins. The repetitive firing during the burst is maintained by the regenerative SIC and by the summation of transient depolarizing afterpotentials or DAPs following each spike. As the burst continues, the $[Ca]_i$ level climbs rapidly because calcium enters with each spike, and the SOC builds up, ultimately terminating the burst. At this point, the cycle begins again.

This model of bursting is not necessarily complete. In the sections to follow, we will discuss possible additions to and changes in this scheme. Very likely, the alterations we suggest will, in time, themselves be altered as new insights to this complex neuronal activity occur.

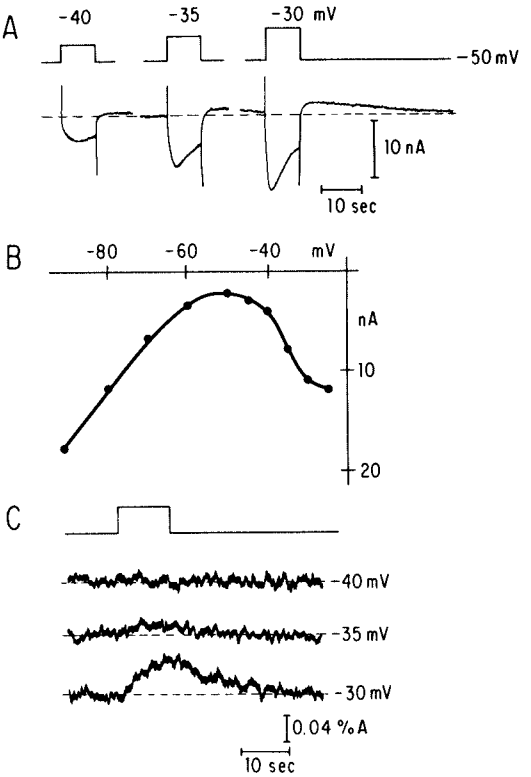

FIG. 2. Slow currents in R15. **A:** Voltage clamp depolarizations disclose slow inward current (SIC) and slow outward current (SOC). **Top traces:** voltage of cell during steps for 10 sec to −40, −35, and −30 mV from holding potential of −50 mV. **Bottom traces:** current (whole cell) during these steps, downward deflection is inward current. Note SIC peaks within 1–5 sec and then begins to relax, more prominently with the larger depolarizations. At these voltages, relaxation is incomplete and longer steps show sustained inward current. After the command, a SOC is seen as a tail current following the steps. The SOC is larger after the greater depolarizations. **B:** The I/V curve of this cell obtained by plotting the peak inward current value versus voltage (holding potential −50 mV). **C: Top trace:** duration and timing of the depolarizing commands given to elicit the SIC. Below it are three traces of the Arsenazo III absorbance at the soma (655–700 nM) during 10-sec depolarizations to −40, −35 and −30 mV. Each absorbance trace is the average of 10 traces (10 depolarizations) to the indicated voltage. The rise of the absorbance signal during the steps to −35 and −30 mV indicate calcium influx produced a detectable rise in $[Ca]_i$ during these commands, whereas at −40 mV no rise in $[Ca]_i$ was detectable. (D. V. Lewis, unpublished data, September 1981.)

IONIC BASIS OF SLOW INWARD CURRENT

In spite of its crucial role in depolarizing the BPN preparatory to the next burst, there is still disagreement about the ionic basis of the SIC. Early experiments demonstrated that elimination or reduction of extracellular sodium reduced or stopped BPA in certain neurons (23, 36,89). This blockage of the slow depolarizing and hyperpolarizing waves of BPA was not simply a result of the blockade of sodium spikes. Cell 11 of *Otala* continued to generate calcium spikes in the absence of sodium (36), and R15 of *Aplysia* generated slow rhythmic depolarizing waves when its spikes were blocked by tetrodotoxin (TTX) and low calcium (89). The sensitivity of BPA to sodium suggested to these investigators that a high resting sodium conductance was responsible for the depolarizing phase of BPA. This sodium conductance was different from that of the spike by being resistant to TTX, and not inactivated by depolarization.

The application of voltage-clamp analysis to BPNs in *Aplysia* and *Otala* added a new dimension to the bursting mechanism, a voltage-sensitive regenerative SIC (20,38,87,93). BPNs seemed to have both a high resting, voltage-insensitive, sodium conductance and a sodium-mediated SIC that was activated by depolarization. The SIC was reduced progressively as the extracellular sodium was reduced and replaced by Tris, lithium, or sucrose (20,87,94). With the elimination of the SIC, the NSR region of the I/V curve was also eliminated, and the I/V curve was identical to that of a nonbursting neuron. The dependence of the SIC on calcium was also tested. Lowering extracellular calcium had not previously blocked BPA (23,36). In voltage-clamp studies, the amplitude of the SIC seemed to vary inversely with the concentration of extracellular calcium. High calcium suppressed the NSR and SIC, whereas low calcium enhanced them (12).

Most of these experiments were performed on BPNs of the molluscan species *Aplysia* and *Otala*. Using *Helix*, a different species of snail, Eckert and Lux (31) suggested that the SIC was carried by calcium ions, not sodium. In *Helix*, elimination of extracellular sodium had little effect on the SIC. Furthermore, the SIC was blocked by calcium blockers such as lanthanum, cobalt, and D-600. Barium, which readily passes through calcium channels (48), enhanced the SIC. Attempts to eliminate extracellular calcium with EGTA were inconclusive because of a marked increase in membrane conductance. It is worth noting that Eckert and Lux (31) utilized a novel voltage-clamp technique. They recorded currents from a small patch of soma membrane by placing a current measuring pipette directly onto the soma. It is uncertain how much differing voltage-clamp techniques contributed to the apparent difference in effects of low sodium on the SIC of *Helix* versus *Aplysia* and *Otala* BPNs.

With the demonstration of a calcium-mediated SIC in *Helix* BPNs, data began to appear suggesting that *Aplysia* BPNs might not have purely sodium-mediated SICs. Addition of calcium channel blockers, manganese, and cobalt to the bathing medium reduced the SIC (and the SOC), and it was suggested that both calcium and sodium carried the SIC in *Aplysia* BPNs (56). A series of elegant studies appeared, using Arsenazo III as an intracellular calcium indicator to monitor calcium influx into invertebrate neurons. Gorman and Thomas (41) clearly demonstrated increases of intracellular calcium in the soma during small prolonged depolarizations that elicited the SIC in R15 of *Aplysia*. The NSR region usually begins between -65 and -55 mV in R15, and Arsenazo III spectrophotometry detected $[Ca]_i$ increments with depolarizations to between -45 and -40 mV or above (41) (Fig. 2C). Smaller calcium influx at more hyperpolarized voltages may occur but could be below the detection limit of the Arsenazo III technique as a result of effective intracellular calcium buffering (42).

Therefore, calcium enters the soma during depolarizations eliciting the SIC, and the SIC is blocked by agents that can block calcium channels; nevertheless, removal of extracellular sodium seems to eliminate the SIC in some BPNs. In a recent paper, Gorman et al. (40) have attempted to resolve this apparent paradox. In experiments using R15 of *Aplysia* exclusively, these investigators placed the neuron in potassium current blockers tetraethylammonium (TEA) and 4-aminopyridine (4-AP) and injected the calcium buffer EGTA intracellularly. Under these conditions, removal of extracellular sodium had minimal effect on the I/V curve of the cell, whereas removal of calcium eliminated the NSR region of the I/V curve. Gorman et al. (40) suggest that removal of extracellular sodium under conditions in which potassium currents are not blocked somehow produces large outward currents that mask the SIC. Thus, the apparent sodium sensitivity of the SIC may actually not be caused by blockade of the SIC, but

rather may represent summation of the SIC with larger outward currents. These authors were also able to demonstrate that SIC varied directly with the extracellular calcium level as the latter was raised or lowered when outward currents were suppressed (TEA and 4-AP) and intracellular calcium accumulation was prevented (intracellular EGTA injection). With this treatment, reduction of extracellular calcium reduced the slope of the NSR region. Again they attribute the previous opposite observations (12) to complex effects of altered extracellular calcium. For example, high extracellular calcium might cause intracellular calcium accumulation and activate calcium-dependent outward potassium currents which would summate with the SIC, eliminating the NSR region of the I/V curve. In addition, high extracellular calcium may alter the surface potential of the outer membrane, shifting the I/V curve such that the SIC is activated at higher apparent depolarizations (52). It appears that much of the difficulty in determining the ionic basis of the SIC could result from the variable amplitude of simultaneous outward potassium currents that occur during the SIC. These currents could change magnitude unbeknownst to the experimenter who is attempting to change only the SIC. This complication has been discussed at length by Lux and Heyer (69) also.

In our view, several questions must be answered before it can be concluded that SICs of BPNs are exclusively calcium mediated. The influx of calcium as measured by Arsenazo III spectrophotometry is first detectable at membrane potentials significantly more depolarized than those at which the SIC first appears (40) (Fig. 2). Does this indicate that a sodium component of the SIC is activated at more hyperpolarized potentials than the calcium component, or that the threshold of the Arsenazo III technique is too high to detect the earliest physiological calcium influx? There also appear to be species differences in the response of BPNs to reduced extracellular sodium (31) and even differences between different BPNs within the same animal (23). Do certain neurons, e.g., R15 of *Aplysia* which is very sensitive to removal of extracellular sodium (12,23,94), have a greater sodium component of the SIC than others, e.g., *Helix* BPNs, which seem insensitive to low sodium? Finally, what is the ionic mechanism and the cause of the hypothetical outward current induced by low extracellular sodium which is proposed (40) to mask the calcium-mediated SIC in *Aplysia* BPNs? It is possible that low sodium causes calcium-activated potassium current by reducing sodium–calcium exchange and causing accumulation of intracellular calcium (30). However, Arsenazo III spectrophotometry has not shown increases of baseline intracellular calcium when R15 is bathed in zero sodium (D. V. Lewis, unpublished observations, June 1982). Neither does low sodium appear to reduce depolarization-induced calcium influx (D. V. Lewis, unpublished observations; 40), whereas, if $[Ca]_i$ were rising in low sodium solutions, one might expect to see reduced calcium influx (33). Until these issues are resolved, it is reasonable to assume that both calcium and sodium may contribute to the SIC.

IONIC BASIS OF SOC

The SOC or slow outward current is found in all BPNs and causes the postburst hyperpolarization. Following either depolarizing voltage-clamp commands or single or multiple spikes, the SOC appears as a slowly peaking (seconds) and very slowly decaying (many seconds) outward current. During the burst of spikes, there is a progressive increase of the SOC that ultimately exceeds the inward current generated during the burst and repolarizes the cell (12, 21,40,75). Activation of the SOC requires an increase in $[Ca]_i$ such as occurs during action potentials or voltage-clamp depolarization (41, 56,66,67,73). The most reasonable explanation of the SOC has been that it represents a calcium-activated potassium conductance. However, recent investigations of this current have suggested that even this accepted explanation may need to be revised.

Early studies of BPNs implicated increased potassium conductance in the termination of the typical bursts of spikes. Junge and Stevens (58) and Gainer (36) suggested that during the postburst hyperpolarization there was a conductance increase that slowly declined as the cell gradually depolarized in advance of the succeeding burst. Periodic injection of identical hyperpolarizing current pulses during the interburst interval was the means used to illustrate the conductance change. However, because of the nonlinear I/V curve of BPNs, this method may give misleading results (47). The voltage change during hyperpolarizing current pulses can be used as an index of voltage-insensitive conductance. However, this deflection can also vary as different voltage sensitive conductances, e.g., the SIC are activated or inactivated during the test pulse itself. For example, as the BPN gradually depolarizes during the interburst interval,

more SIC is turned on as the membrane potential enters the region of decreasing positive slope, just preceding the NSR region of the I/V curve. A brief hyperpolarizing current pulse at this potential will inactivate some SIC, resulting in an augmented voltage deflection during the pulse. This phenomenon would cause increasing deflections with successive current pulses during the interburst interval, resembling what could also be seen during the gradual decay of a voltage-insensitive potassium conductance. Still using current clamp methods, Junge and Stevens (58) seemed to be able to reverse the postburst hyperpolarization to a depolarization with the constant injection of a large hyperpolarizing current. In addition, the reversal potential was sensitive to changes in extracellular potassium as expected of a potassium conductance. Carnevale (20), Gola (38) and Smith et al. (87) used voltage clamp to study the SOC following spikes or voltage-clamp depolarizations. All found the current to decrease in amplitude with hyperpolarization and to be sensitive to changes in extracellular potassium. Some demonstrated inversion of the SOC near the potassium equilibrium potential (12), whereas in other studies inversion was not attained (20,57). It should be mentioned that activation of an electrogenic sodium pump had also been considered as a possible mechanism of the SOC or postburst hyperpolarization (89). However, this hypothesis was abandoned when pump blockers and metabolic poisons failed to eliminate the postburst hyperpolarization (20,22,58).

While the SOC was being characterized as a potassium current, other investigators were demonstrating that calcium injection into molluscan and vertebrate neurons also elicited potassium current (63,72). Stinnakre and Tauc (88), using the calcium indicator aequorin, showed marked rises in $[Ca]_i$ during spikes in R15 of *Aplysia*. It was logical to suggest that the SOC was a calcium-activated potassium conductance (58) such as that described by Meech (72) in *Aplysia* neurons. Subsequent voltage-clamp studies clearly demonstrated that depolarization sufficient to produce large calcium influx activated outward potassium currents (28,33,51, 57,76). The potassium current was clearly dependent upon calcium influx because calcium channel blockers and depolarizing commands exceeding the calcium equilibrium potential eliminated it. In addition, buffering the increases in $[Ca]_i$ by intracellular injection of EGTA appeared to eliminate the component of potassium current attributed to calcium influx (28,64,75). Using intracellular calcium indicators, the increase in potassium conductance was found to correlate with the increase in $[Ca]_i$ during and after voltage-clamp commands (4,32,43).

These investigations produced general agreement that calcium activates potassium currents, although some disagreement remains on the details of this system. Most investigators think that the rise of $[Ca]_i$ at the inner membrane surface increases the potassium conductance, resulting in the delayed potassium current seen during depolarizing commands and causing the slowly decaying outward currents after a train of spikes (4,28,32,43,56,64,68,75). However, Lux and Heyer (69) have presented a significantly different interpretation. Using an extracellular potassium-sensitive microelectrode to monitor potassium efflux, these investigators have concluded that it is the actual passage of calcium through the membrane that activates the delayed potassium current seen during depolarizing commands. Thus, the passage of calcium through the membrane rather than the resultant rise in $[Ca]_i$ activates a potassium conductance. Lux and Heyer (69) suggest that the current activated by increased $[Ca]_i$ is a different potassium current, a potassium leakage (not time-dependent) current. Although this issue may not yet be entirely resolved, we make the simplifying assumption that there is one calcium-activated potassium conductance, and that it is activated by increased $[Ca]_i$ rather than by transmembrane calcium flux.

Returning to the role of calcium-activated potassium currents in BPA, Gorman and Thomas (41) used Arsenazo III spectrophotometry to follow changes in $[Ca]_i$ in R15 during the bursting cycle (Fig. 1). They illustrated marked rises in $[Ca]_i$ during the burst and slow decline of $[Ca]_i$ during the interburst interval (Fig. 1). Thus, there existed abundant evidence that increased $[Ca]_i$ activated a potassium conductance in BPNs, and that $[Ca]_i$ increased during a burst. However, there was little direct and conclusive evidence that the postburst hyperpolarization resulted entirely from the calcium-activated potassium current. In fact, the demonstration that intracellular calcium accumulation might inactivate inward calcium currents (33) prompted speculation that a component of the postburst hyperpolarization might be caused by a calcium-mediated inactivation of the SIC (92).

Within the last several years, evidence suggesting that inactivation of inward current, most probably the SIC, may account for the SOC and the postburst hyperpolarization has been inde-

pendently presented by several investigators (1,61,62,67). These experiments, using *Aplysia* BPNs, have shown no inversion of the SOC at hyperpolarized holding potentials well below the presumed potassium equilibrium potential, nor sensitivity of the SOC to altered extracellular potassium concentration. Another source of evidence that the SOC may not be a calcium-activated potassium current is its insensitivity to TEA. Although there has been some disagreement (90), several investigators have shown that extracellular TEA will block the potassium currents elicited by either intracellular calcium injection or calcium influx during large depolarizing commands (1,50,61,62,76) in *Aplysia* and *Helix* neurons. However, at least in *Aplysia* neurons, TEA does not block the prolonged outward tail currents or SOC following calcium influx during depolarization (1,61,62).

Therefore, although the SOC followed depolarization-induced calcium influx, it did not have the properties expected of a potassium current. There was no question, however, that the SOC was dependent upon an increase in $[Ca]_i$. It was eliminated by intracellular EGTA, depolarization to voltages exceeding the calcium equilibrium potential did not elicit an SOC, and the SOC was blocked by calcium channel blockers or by elimination of extracellular calcium. The interpretation of these data was the same by several groups (1,61,62,67); the SOC represented, in BPNs, a calcium-mediated inactivation of a persistent inward current. The inward current being inactivated appeared to be identical to the SIC. The voltage sensitivity of the SOC agrees with the voltage activation characteristics of the SIC. At hyperpolarized potentials at which the SOC is small, very little SIC is tonically activated; thus, there is very little to inactivate. At depolarized potentials at which most SIC is tonically activated, the SOC is larger, there being more SIC to be inactivated by calcium influx.

Given the clear presence of calcium-activated potassium channels and the marked increase in intracellular calcium during a burst, it seems premature to conclude that the SOC underlying the postburst hyperpolarization has no component of potassium conductance. We have discussed evidence that under some circumstances the SOC seemed sensitive to altered extracellular potassium. The explanation for conflicting data is not clear. The outstanding conflicting observations seem to involve the response of the SOC to altered extracellular potassium and whether or not the SOC reverses at hyperpolarized potentials. Very likely, the slow outward tail currents following depolarization of BPNs, collectively referred to as the SOC, can be composed of varying proportions of SIC inactivation and calcium-activated potassium current, with the relative proportions determined by differing experimental techniques and biological factors. Obviously, these concepts are still evolving, and it may be some time before the final answer will be known.

CALCIUM-ACTIVATED INWARD CURRENTS IN BPNs

As discussed above, numerous studies have shown that pressure injection or iontophoresis of calcium intracellularly in BPNs and other neurons produces outward potassium currents (17,39,63,72,74). Occasionally, there has been mention of calcium injection producing transient inward currents as well. Meech (74) pressure-injected calcium salts into *Helix* neurons and observed occasional biphasic responses consisting of an early transient depolarization followed by a prolonged hyperpolarization. With smaller injections, only hyperpolarizing potassium-mediated responses were observed. While pressure-injecting calcium into the nonbursting neuron R2 of *Aplysia,* Brown and Brown (17) noted that very large injections occasionally caused initial depolarization followed by prolonged hyperpolarization. Hofmeier and Lux (53) extensively studied the inward current associated with calcium injection and proposed that it was not an artifact of excessive calcium injection but reflected a physiological effect of normal calcium influx. By pressure-injection of calcium in *Helix* BPNs, they could consistently elicit a transient inward current peaking in several seconds, followed by a more prolonged outward current peaking many seconds later. The inward current was increased by hyperpolarization, was associated with a simultaneous conductance increase, and had an extrapolated reversal potential between -20 and $+20$ mV. Nickel, an effective calcium channel blocker, did not eliminate the inward current, nor did replacement of extracellular sodium with sucrose; therefore, the ionic basis of the current was unclear. The authors speculated that previous studies elicited primarily outward currents because calcium was injected or iontophoresed intracellularly in smaller amounts and relatively slowly. They surmised that rapid, large injections were required to raise $[Ca]_i$ sufficiently at the inner membrane surface to activate the inward current. By reducing the size of their cal-

cium injections, Hofmeier and Lux (53) could elicit pure outward current responses.

The physiological role of calcium activated inward currents in BPNs is also being clarified. Following spikes in BPNs are prominent depolarizing afterpotentials or DAPs (91) which precede the later-occurring, previously discussed, SOC or hyperpolarizing aftercurrent (Fig. 3). Lewis (66) presented evidence that DAPs in R15 of *Aplysia* might be activated by increased $[Ca]_i$. DAP current was very sensitive to reduced extracellular calcium, calcium channel blockers, and intracellular injection of calcium buffers EGTA or EDTA. The ionic conductance underlying DAPs had many similarities to the SIC, and Lewis (66) suggested that DAPs might arise from a calcium-mediated activation of the SIC.

A calcium-activated inward current has also been studied by Kramer (61) in left upper quadrant BPNs in *Aplysia,* which, like R15, are in the abdominal ganglion. This current causes DAPs in these neurons and shows the same dependence upon increased $[Ca]_i$ as the DAP current described by Lewis (66). In addition, Kramer (61) was able to show that the current was not activated by depolarizing commands that exceeded the calcium equilibrium potential, thus further excluding any role of depolarization per se in activating it. Kramer (61) also demonstrated that calcium iontophoresis intracellularly in these BPNs activated a voltage-independent inward current that could be seen when the superimposed larger outward potassium current (39) was blocked by extracellular TEA. This observation has been repeated in R15 by Lewis (unpublished observations, December 1983). Kramer suggests that both the DAP current and the inward current activated by calcium injection are identical and are examples of the nonselective calcium-activated cation channels found in neuroblastoma, cardiac cells, and pancreatic acinar cells (27,70,96).

An alternative interpretation of the DAP current has been offered by Adams and Levitan (2) working with R15. These investigators suggest that DAPs result from electronic spread of action potential currents from the axon. They note that axotomy of R15 eliminates DAPs, and that, like the action potentials of R15, the DAPs are dependent upon both extracellular sodium and calcium.

We suggest that the increasing evidence for calcium-activated inward currents in BPNs justifies adding this mechanism to the model of BPA. Previous concepts of the DAP were that it is simply a manifestation of the SIC, and therefore its role in producing bursting activity was lumped with the role of the SIC (47). However, if the DAP current is a calcium-activated inward current, it is therefore removed from the cate-

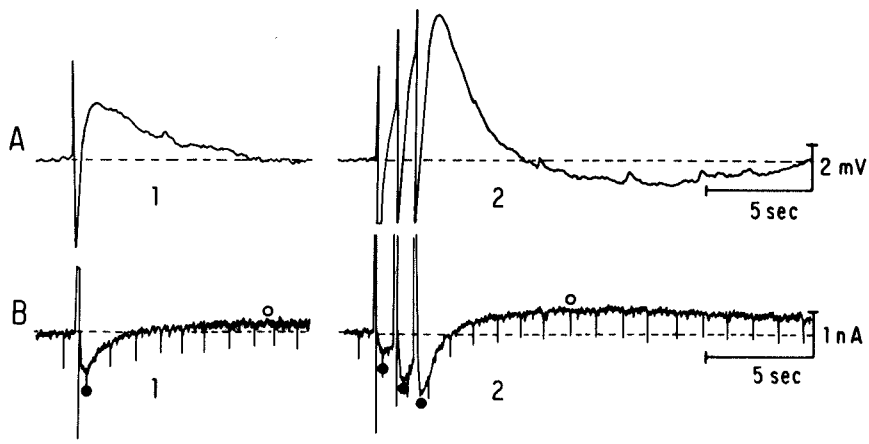

FIG. 3. Depolarizing after potentials in R15. **A1**: R15 in current clamp at −59 mV showing the DAP after one spike triggered by a 5-msec pulse of depolarizing current. The initial positive (*upward*) deflection is the spike (overshoot is clipped by the pen recorder), the following negative (*downward*) deflection is the spike undershoot and the final prolonged positive deflection is the DAP. **A2**: By triggering three consecutive spikes, summation of DAPs can be observed; following the DAPs, a prolonged hyperpolarization reflecting the SOC can be seen. **B1**: By placing the cell in voltage clamp, except for a brief 50-msec interval when the spike is triggered, the currents underlying the DAP (●) and the succeeding hyperpolarization (○) can be measured after one (**B1**) or several (**B2**) spikes. The prolonged outward current (○) following the DAP current is the SOC. Monophasic downward deflections in **B** are excitatory postsynaptic currents. From Lewis, ref. 66, with permission.

gory of simply a manifestation of the voltage-activated SIC and there is a need for further consideration of its role in BPA.

EXPANDED MODEL OF BPA

Here we will attempt to incorporate several additional mechanisms into the previously described model of bursting based on the SIC and SOC. The additional features will be the role of DAPs in initiating and maintaining the burst (91), the activation of inward DAP current by increased $[Ca]_i$ (61,66) and the inactivation of inward current by increased $[Ca]_i$ (1,61,62,67). We stress that any model of bursting must be considered tentative, awaiting new research in this area. Furthermore, the suggested role of $[Ca]_i$ in activation and inactivation of inward currents during BPA has yet to be observed in species other than *Aplysia* and *Helix*. Therefore, this is not intended to be a generalized model of BPA; there are undoubtedly many other existing mechanisms of BPA just as there are other neurons exhibiting bursting behavior.

The importance of DAPs in BPA was stressed by Thompson and Smith (91) in a study of BPNs from *Archidoris, Anisodoris, Aplysia, Helix,* and *Tritonia*. Spikes in these cells were followed by DAPs that were seconds in duration. Thompson and Smith showed that DAPs from successive spikes underwent temporal summation (Fig. 3) creating a significant depolarizing current that very likely had a role in maintaining the burst of spikes and causing the acceleration of firing rate typically seen in the initial half of a burst. We agree that DAP currents have a significant role in many BPNs and suggest that reconsideration of DAP function is warranted by recent suggestions that DAPs may represent calcium-activated inward currents.

The sequence of inward and then outward aftercurrents activated by the calcium influx during spikes in BPNs seems ideally suited to support BPA. As seen in Fig. 3, the DAP current is larger and briefer than the following SOC, and both aftercurrents show temporal summation (66,91). A very rough approximation of the way in which these aftercurrents might summate during a burst to produce the initial acceleration of spiking, then deceleration and cessation of the burst, can be illustrated by attempting to imitate a burst with voltage-clamp commands (Fig. 4). A spike-like depolarization of the cell, e.g., a command to +40 msec for 15 msec, will elicit a DAP current and subsequent SOC similar to those following a spike. By delivering a train of

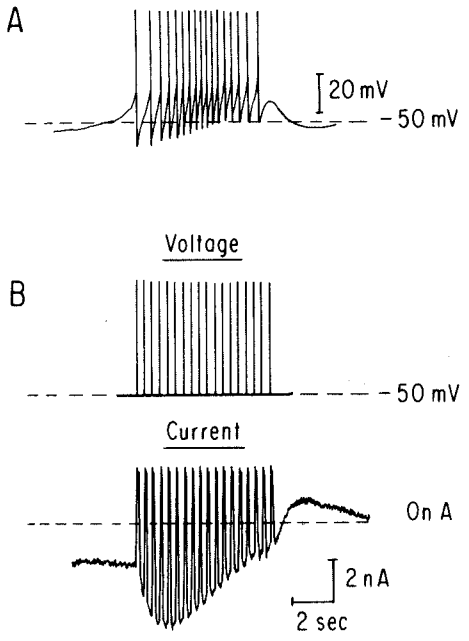

FIG. 4. Burst structure and summation of spike aftercurrents. **A:** R15 was allowed to burst spontaneously. The typical burst illustrated here contained 18 spikes and demonstrates the increasing and then the decreasing spike firing rate followed by the interburst hyperpolarization. **B:** A simulation of a burst was attempted with the cell in voltage clamp. **Upper trace:** (voltage) shows the train of 17 depolarizing steps to +40 mV for 15 msec, each from a holding potential of −50 mV. **Lower trace:** (current) shows the current trace during the train of depolarizing commands (the large brief outward currents during the commands are clipped by limited pen recorder motion). Note that the baseline net membrane current initially becomes more inward and then shifts in an outward direction, becoming briefly net outward at the end of the train. (D. V. Lewis, unpublished data, June 1984.)

such depolarizations, one can observe an initial increase of net inward current followed by a gradual decrease of net inward current and, ultimately, a net outward current. This same sequence probably occurs during a spontaneous burst, causing the initial acceleration, then deceleration, and cessation of spiking typical of a burst.

In summary, we think an expanded model of BPA is appropriate at this time (Fig. 5). Beginning at the nadir of hyperpolarization following a burst, $[Ca]_i$ has been elevated by the burst and has inactivated a significant proportion of the SIC and activated an unknown amount of calcium-dependent potassium current. As the $[Ca]_i$ declines during the interburst interval, the SIC is reactivated and the potassium conductance

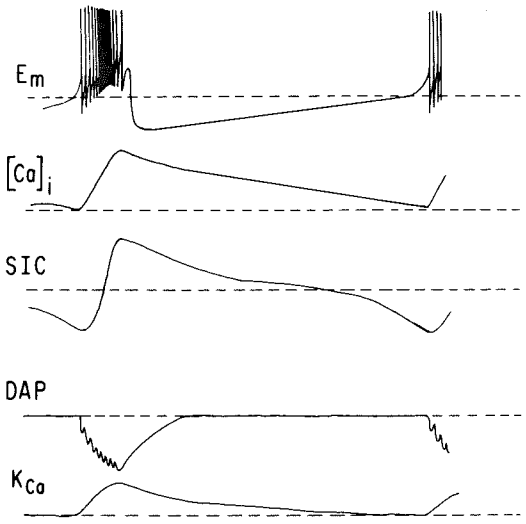

FIG. 5. Illustration of hypothetical model of bursting pacemaker activity. Em, membrane voltage; $[Ca]_i$, intracellular calcium activity measured at the soma. This represents average $[Ca]_i$ as seen with Arsenazo III; here the rise in $[Ca]_i$ is depicted as a smooth rise, but with optimal records it can be seen to increment in a pulsatile manner with each spike, e.g., Gorman and Thomas (41). SIC, slow inward current (a decrease in SIC is depicted as an upward deflection); DAP, summating DAP currents which are inward, hence downward deflection; K_{Ca}, calcium activated potassium current. The time courses of inactivation of the SIC, decay of the DAP currents, and increase and decline of K_{Ca} are at this point uncertain. The traces are illustrative only and should not be taken to represent actual current magnitudes. Baselines are also relative and in the case of the SIC do not represent zero current level.

decreases. This causes depolarization, which in turn activates more SIC, driving the depolarization incessantly toward spike threshold. During the first spike, there is a marked increase in $[Ca]_i$ at the inner membrane surface, and the DAP is activated, bringing the cell out of the spike undershoot and to threshold for the next spike. The DAPs summate and accelerate the spiking. With a slight delay, the increased $[Ca]_i$ begins to inactivate the SIC and perhaps to activate a potassium conductance. These combined features decelerate spiking and terminate the burst, and the cycle begins again.

MODULATION OF BURSTING PACEMAKER ACTIVITY BY NEUROTRANSMITTERS

The currents generating BPA are, in the neurons discussed above, nonsynaptic and endogenous to the BPN membrane. However, neurotransmitters and other neuroregulators can alter BPA either by controlling the voltage-sensitive SIC or by superimposing discrete postsynaptic currents which transiently accelerate or retard a burst. A large number of interesting studies exist concerning modulation of BPA by exogenous peptides and steroids (11), endogenous peptides (71), and spontaneous synaptic input (79,82). Synaptic input can either inhibit or enhance BPA. Inhibition of long duration will stop BPA in R15 for many minutes (3,79). Stimulation of the right pleurovisceral connective can enhance BPA for hours in R15 (79). Synaptic input can also induce BPA in silent neurons, as in the lobster stomatogastric ganglion in which neurons will generate BPA only when afferent input is intact even though the BPA is not caused by discrete postsynaptic currents (7,77). As with nonbursting neurons, cyclic nucleotides may often be the intracellular messengers mediating the effects of the neurotransmitters on BPA (65).

This brief review cannot adequately encompass the literature on neuroregulators and BPA. Therefore, we will focus on one example of such modulation, the inhibition of BPA in R15 by dopamine. Dopamine is found in high concentrations in molluscan nervous tissue, including that of *Aplysia* (44). Ascher (9) characterized the dopamine responses of multiple neurons of *Aplysia*. Dopamine application was effective on the axons rather than the somata and had both inhibitory and excitatory effects. The response of the BPN R15 was purely hyperpolarizing and, unlike most of the other hyperpolarizing responses, was not inverted by hyperpolarization to below the presumed potassium equilibrium potential, nor was it sensitive to alterations in extracellular potassium. However, with the application of sodium pump inhibitors and with cooling, the response appeared to invert near -90 mV, and the inversion became sensitive to extracellular potassium. These and other considerations led Ascher (9) to propose that dopamine was increasing potassium conductance in R15, thus hyperpolarizing the cell and stopping bursting. To explain the failure of the dopamine response to invert under normal conditions, Ascher (9) speculated that the site of dopamine action was electrically distant from the soma and therefore difficult to invert with hyperpolarization at the soma. He further speculated that the extracellular surface of R15 was protected from changes in extracellular potassium by an unspecified diffusion barrier, explaining the insensitivity of the dopamine response to altered extracellular potassium.

Wilson and Wachtel (94) proposed the alternative interpretation that dopamine was blocking the regenerative SIC. They iontophoresed dopamine onto the axodendritic region of the cell and eliminated the NSR region of the I/V curve without increasing conductance in the hyperpolarized voltage range. Transient outward shifts of membrane current elicited by dopamine iontophoresis were not affected by increasing extracellular potassium, but were eliminated by removing extracellular sodium which also eliminated the SIC and NSR region of the I/V curve. These observations suggested that dopamine was blocking the voltage-sensitive SIC. Furthermore, when BPA was blocked by bath-applied dopamine, injection of depolarizing current could not restore bursting, arguing that dopamine was not simply superimposing a constant hyperpolarizing current (45). Gospe and Wilson (45) established a dose–response curve for the effect of bath applied dopamine on the I/V curve of R15 showing maximum effect at 500 μM. The dopamine effect was antagonized by dihydroergotamine and lysergic acid diethylamide, but not by neuroleptics or certain adrenergic antagonists. Therefore, Gospe and Wilson (46) concluded that the receptor mediating BPA inhibition in R15 was different from previously described dopamine receptors.

Adams et al. (3) compared the effects of branchial nerve stimulation to those of dopamine application. In R15, branchial nerve stimulation produced an outward current that had two components. The early component was associated with a slope conductance increase resembling a potassium conductance. The late component was a reduction in the NSR without a conductance increase in the hyperpolarized limb of the I/V curve. Dopamine application eliminated the late but not the early component. Adams et al. interpreted these results as indicating that both the dopamine effect and the late component of branchial nerve stimulation resulted from elimination of the SIC and that they therefore occluded one another.

Understanding the action of dopamine, as with the SIC and SOC, seemed to hinge upon the differentiation of increased outward current from decreased inward current. Lewis et al. (67) attempted to overcome this dilemma, at least insofar as calcium influx was concerned, by using Arsenazo III spectrophotometry. During small, subthreshold depolarizations, in the range of the SIC, a rise in $[Ca]_i$ was seen in the soma of R15. A maximum dopamine concentration of 500 μM did not reduce the rise in $[Ca]_i$ at the soma. Next, axodendritic absorbance changes were monitored, and rises in $[Ca]_i$ in the axon region could also be seen during the activation of the SIC. In the axodendritic region, dopamine markedly attenuated the $[Ca]_i$ rise. It appeared that, just as dopamine application is only effective in the axodendritic region in producing current responses, so is it effective in reducing axodendritic, but not somatic, calcium influx. During voltage clamp, simultaneous voltage measurements in the soma and axon showed that dopamine application had little effect on voltage control in the axon, suggesting that the decreased calcium influx resulted from a decrease in calcium conductance rather than from altered space clamp properties.

Recently, dopamine has been shown to affect not only the SIC, but the DAP current (66) and the SOC (67) as well (Fig. 6). DAP currents following single spikes and voltage-clamp commands are reduced and ultimately eliminated by dopamine in a dose-dependent manner (66). The effect of dopamine on the DAP current is equally effective whether the dopamine is bath-applied or applied locally to the axodendritic region, but is not seen when dopamine is applied locally to the soma. One could speculate therefore, that dopamine may reduce the DAP by reducing axodendritic calcium influx during a spike.

Dopamine effects on the SOC are more complex. Low concentrations of dopamine will increase the magnitude of the outward current following a train of action potentials in R15 (8) (Fig. 7A). However, after single or very few spikes or after a brief depolarizing command, dopamine reduces the SOC (Fig. 6). The explanation of these apparently contradictory observations is not yet known. Possibly the currents contributing to the SOC after a burst of spikes are different from those comprising the SOC after one spike. Furthermore, since the net posttetanic current after a burst of spikes may reflect algebraic summation of several different currents including DAP currents, inactivation of SIC, and calcium-activated potassium current, the exact cause of a change in the net current will be difficult to ascertain.

It would be ideal to account for all of the effects of dopamine with one unifying hypothesis. An attractive hypothesis would be that dopamine reduces voltage-sensitive axodendritic calcium influx. This would explain the reduction of the SIC, the reduced calcium dependent DAPs, and decreased SOC. However, it will not explain the increased posttetanic current following a long burst of spikes. Clearly, more effort is re-

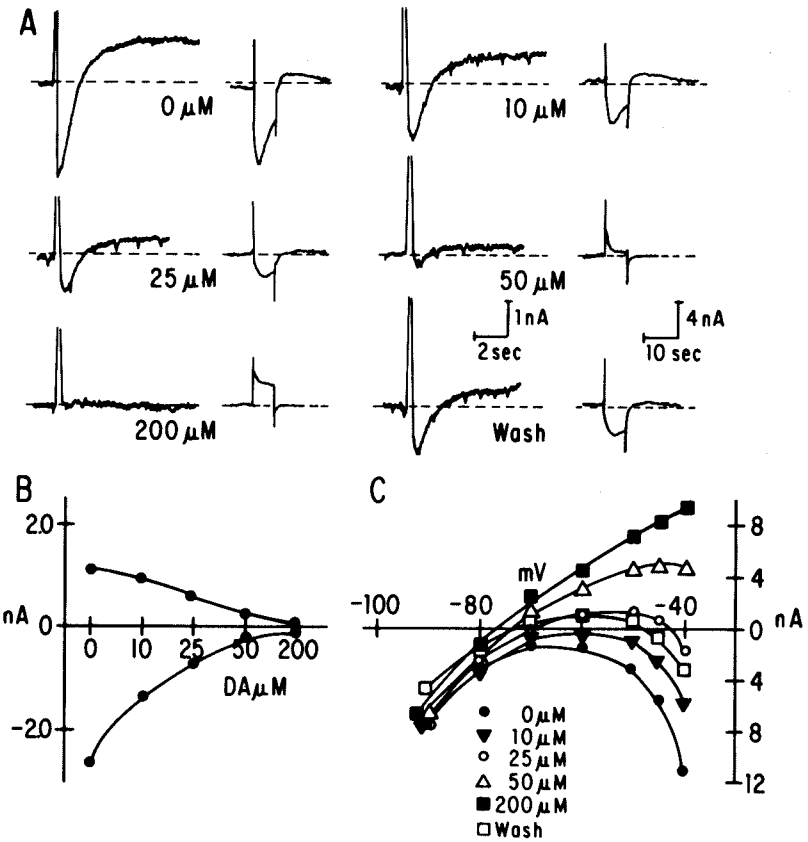

FIG. 6. Dopamine effects on membrane currents in R15. A: These current traces show the concentration-dependent effects of dopamine on the DAP current, and the slow outward and slow inward currents (SOC and SIC). Six pairs of traces are illustrated, each consisting of one trace (*left*) of the inward DAP current and SOC following one spike (cell placed in voltage clamp at −50 mV after the spike) and one trace (*right*) of the SIC and following SOC activated by a depolarization from −50 to −40 mV for 8 sec. Before dopamine exposure (0 μM), the usual currents are present. With progressively higher dopamine concentration in the bath, the DAP current, SOC following the DAP current, the SIC, and the SOC following the SIC are all eliminated. Partial recovery follows the wash. Often, after prolonged exposure to high concentrations (as in this example) of dopamine recovery is incomplete or takes several hours. **B:** Graph of the amplitude of the DAP current (*lower curve*) and of the SOC (after one spike) (*upper curve*) versus dopamine concentration in the bath. C: I/V curves of the cell in the various concentrations of dopamine (holding potential −50 mV, current at 1.5 sec after beginning of command). From Lewis, ref. 66, with permission.

quired to explain all these phenomena. It is of interest in this regard that dopamine application to hippocampal pyramidal cells increases the hyperpolarization following a train of spikes (16). Even lacking a full understanding of the mechanisms, knowing the diversity of the dopamine effects helps to clarify the ways in which this neurotransmitter could modulate BPA. Reducing the SIC would tend to prevent regenerative depolarization of the cell. Reducing the DAP current would tend to reduce the depolarizing drive during a burst, hence reducing spike frequency during the burst; enhancing the SOC generated during a burst would also tend to shorten the burst. Indeed, the most clear-cut effect of low concentrations of dopamine is to reduce the number of spikes per burst and increase the interspike intervals (Fig. 7B), whereas higher concentrations halt BPA entirely.

CONCLUSION

From this synthesis of the studies of burst-firing neurons, it is clear that what seemed initially to be a quite simple process is actually much more complicated. The regulation of burst firing by neurotransmitters, such as dopamine regulation of bursting in R15, has proven much

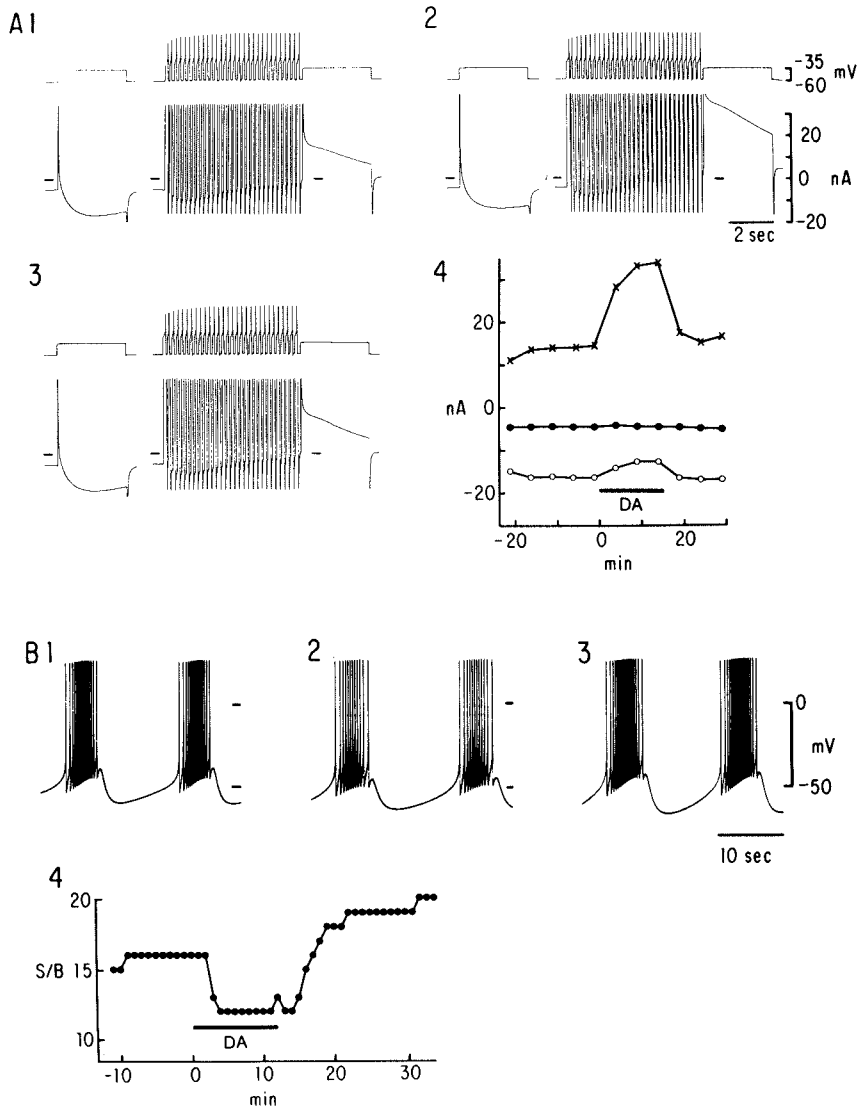

FIG. 7. **A:** Enhancement of spike-evoked slow outward current (SOC) in neuron R15 by a low concentration of dopamine. Every 30 sec, the cell was depolarized from a holding potential of −60 mV to a pulse voltage of −35 mV for 3 sec, which produced a persistent slow inward current (SIC). Every 5 min (i.e., every 10th pulse), a 5.8-sec, 5.0-Hz train of action potentials (in current clamp) preceded the depolarizing clamp pulse, which now produced a SOC. **A1:** Normal saline control. The SIC during a depolarizing clamp pulse (*left*) was converted to a SOC following a train of spikes (right). **A2:** In 5 μM dopamine, the inward current was reduced slightly (*left*) as compared with control values, but the SOC following the spike train (*right*) was doubled. The increase in SOC was five times the decrease in SIC. **A3:** Recovery in normal saline. **A4:** Plot of the experiment in A1–A3. Solid circles, holding current; open circles, peak SIC; Xs, SOC. **B:** The effect of a low concentration of dopamine on spontaneous bursting in R15. **B1:** Normal saline control; **B2:** 5 μM dopamine. There was a 25% decrease in spikes/burst, and a 43% increase in mean interspike interval. **B3:** Recovery in normal saline. **B4:** Plot of spikes/burst (S/B) from the experiment in **B1–B3.** **A** and **B** are from different preparations. (W. W. Anderson, unpublished observations, April 1984.)

more difficult to analyze than are more conventional synaptic processes.

Because analogies are often drawn between invertebrate burst-firing neurons and neurons participating in epileptogenic activity, it is appropriate to recognize the complexity of these neuronal burst-firing processes. Even in cells as amenable to study as the *Aplysia* neurons, the

data can be complex and, at times, confusing. The situation is much more difficult in the mammalian central nervous system (CNS), and extreme caution would be appropriate in the interpretation of experiments to study bursting in these cells.

SPIKE FREQUENCY ADAPTATION

Spike frequency adaptation (SFA), or accommodation, is the process in which a neuron responds to a constant stimulus with a decreasing rate of firing of action potentials. The result of this process is that the firing rate of a neuron is more closely related to the rate of change of the stimulus than to the steady state level of the stimulus. It seems plausible to postulate that the process of SFA may be an endogenous "anticonvulsant" mechanism in certain neurons, and that the suppression of SFA might promote epileptiform activity. This hypothesis is based on the assumption that seizures are related to the supranormal activity of certain foci in the CNS, and that a decrease in the ability of individual neurons to sustain a high level of activity may help to prevent either the initiation of a seizure focus or the spread of activity from the seizure focus to other areas of the CNS.

Adaptation is a somewhat universal phenomenon in neurophysiology. Not only has it been extensively studied in invertebrates (25,80,81), but it has also been demonstrated in the mammalian CNS, with adaptation responses having been shown in the spinal cord (10,55,59,60).

Several mechanisms that contribute to the process of adaptation have been elucidated. In general, these mechanisms have a slow hyperpolarizing effect on the membrane during a train of action potentials that leads to increasing interspike intervals. Baylor and Nichols (15) demonstrated a prolonged hyperpolarization after a train of spike in leech sensory neurons. The hyperpolarization was blocked by cooling and the cardiac glycosides, ouabain and strophanthidin, and therefore was attributed to the action of an electrogenic pump. Brodwick and Junge (19) studied a posttetanic hyperpolarization in *Aplysia* giant neuron R2. They showed that the hyperpolarization was not blocked by inhibitors of electrogenic pumping (cooling, ouabain, cyanide, and removal of extracellular Na^+ or K^+), but instead was caused by an increase in potassium conductance. Furthermore, since the hyperpolarization persisted in the absence of action potentials (blocked by TTX), it could not be accounted for by the summation of spike afterhyperpolarizations. Partridge and Stevens (81) were able to show that a SOC of this type could account for adaptation in the marine molluscs *Archidoris* and *Anisodoris*. In response to a constant current step, these neurons showed an adapting response. However, when Partridge and Stevens superimposed an exponentially rising current onto the constant current step, they were able to "frequency clamp" the cell. That is, they blocked adaptation by negating the effects of a SOC. Using this method, they were able to explain adaptation in these cells.

Colmers et al. (26) showed that in the presence of Cs^+ (a blocker of K^+ currents), there is a net inward current in response to subthreshold depolarizations in *Aplysia* giant neurons. The activation of this inward current would result in an increase in firing rate of a neuron. The inward current inactivates somewhat during the first 5–10 sec of depolarization of the membrane. Therefore, this process may also contribute to adaptation.

Lewis and Wilson (68) have demonstrated another mechanism that is important in early adaptation. Using the calcium-sensitive dye, Arsenazo III, in conjunction with differential absorbance spectrophotometry, they were able to measure changes in the intracellular levels of Ca^{2+} in *Aplysia* giant neurons. They showed that during the first 5–10 sec of an adaptation response, there is a rapid increase in intracellular Ca^{2+}, and that this portion of adaptation could be accounted for by the onset of a Ca^{2+}-activated K^+ conductance.

Cote et al. (29) used a voltage-clamp analysis to study a SOC in *Aplysia* giant neurons. They showed that the SOC was a potassium current that was activated by subthreshold depolarizations, that the current could account for adaptation, and that the current was enhanced by submillimolar concentrations of barbiturates (pentobarbital and phenobarbital). It has been further proposed that enhancement of SOC by barbiturates is an anticonvulsant effect (97).

The phenomenon of spike frequency adaptation and the effect of an anticonvulsant barbiturate on it is shown in Fig. 8. In this case, diphenylbarbituric acid (DPB) (54,85) was used to enhance SFA. Adaptation in these cells occurs in two phases. In response to a constant depolarizing stimulus current (indicated by the arrows in Fig. 8) the firing of the cell declines rapidly at first, and then slowly. This is best seen in part B of the figure in which the interspike interval is plotted versus time. In control artificial seawater (ASW), the interspike interval in-

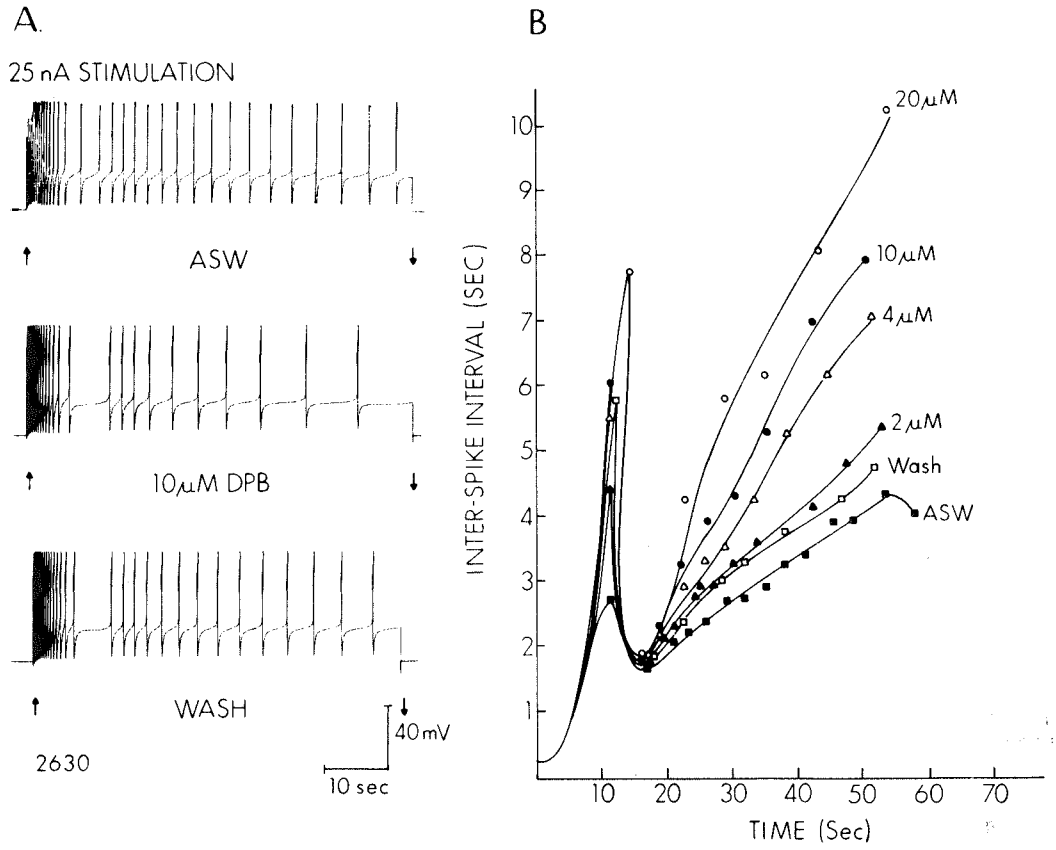

FIG. 8. Typical repetitive firing pattern of giant cell R2, and changes produced by DPB. **A**: Adaptation in response to a 60-sec, 25-nA constant current depolarization obtained in control, with 10 μM DPB, and with wash. Arrows mark the beginning and end of the stimulus. **B**: To elucidate the relationship between DPB concentration and adaptation, data from the experiment in part **A** are plotted as the interspike interval (ISI) versus time of depolarization. DPB causes a dose-related, reversible increase in adaptation as evidenced by an increased rate of development of ISI. Adaptation within the first 5 sec was unchanged by DPB. From Huguenard and Wilson, ref. 54, with permission.

creases rapidly during the first few seconds of stimulation, and then increases more slowly as the stimulus is maintained. DPB enhances the slow adaptation process, without altering the firing rate during the first few seconds, as is best seen in Fig. 8A.

The fast phase of adaptation appears to be the direct result of a calcium-activated potassium current (68), and is not sensitive to barbiturates (97). Therefore, we have concentrated our efforts on understanding the slow phase of adaptation, which is barbiturate enhanced. In this review, we explain how we have studied this process and the membrane current underlying it. We present some additional data implicating potassium as the primary current carrier for the SOC producing the slow phase of SFA, discuss the unusual sensitivity of the process to calcium, and then present an admittedly speculative model describing the process.

Our previous studies linked a SOC (as shown in Fig. 9) to the slow phase of SFA (97) and provided a qualitative description of the effects of barbiturates on this current. However, to study this SOC and the effects of drugs on it thoroughly, an accurate means of quantitating the current is necessary. Unfortunately, there are a number of problems involved in directly measuring the onset of SOC. First, the study by Colmers et al. (26) showed that during the initial 5 sec of a subthreshold depolarization, there is an activation and a partial inactivation of an inward current. These changes in the inward current are occurring at a time course similar to the initial changes in SOC. Therefore, one cannot use the change in whole cell current during a

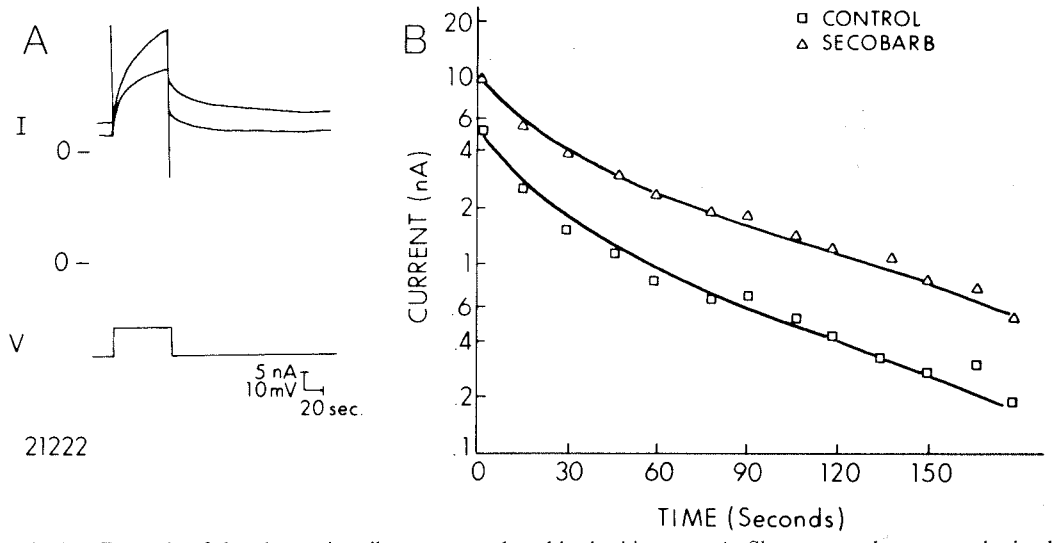

FIG. 9. Example of the change in tail current produced by barbiturates: **A:** Slow outward currents obtained in control and with 100 μM secobarbital. *Upper trace;* current (up, outward); *lower trace;* voltage. **B:** Semilog plots of tail currents from part **A.** Stimulus, 60-sec depolarization to −34 mV from a holding potential of −50 mV.

depolarizing pulse as a measure of the change in outward current. Second, the rise in SOC is an extremely slow process; depolarizations of up to 30–40 min are required even to approach a maximum effect. The slope of SOC during the first 60 sec of depolarization represents less than 5% of the total SOC activation curve. With this limited sample of the time course of activation, it is difficult to determine accurately the parameters describing the process.

Considering the difficulties involved in analyzing the onset of SOC, alternatives must be considered. A good option is the analysis of "tail currents," the decay of a stimulus-induced current; in this case, the stimulus was SOC. Upon repolarization to the holding potential after SOC activation, there was a very slow return of the current to baseline levels. After some initial studies, which showed that tail currents could easily be represented by the sum of exponential decay processes, it was decided that tail current analysis was suitable for the quantitation of SOC.

Analysis of tail currents has several advantages over analysis of the SOC itself. First, with a stable holding current, the endpoint of decay is known. This greatly simplifies the analysis of an exponential decay process. Second, since the tails could be represented as the sum of exponential decay processes, we could use simple, readily available analysis routines to determine the parameters of decay. Last, it was found quite early in this study that barbiturate-induced changes in SOC correlated very well with changes in the parameters describing tail currents. Therefore, tail current analysis provided a means to measure accurately and reproducibly (albeit indirectly) barbiturate-induced changes in SOC.

EXPERIMENTAL DESIGN

Preparation

The giant cells of *Aplysia* were chosen for this study for several reasons. Homologous cells LP1 and R2 are extremely easy to identify, and the membrane properties in these neurons are very constant from preparation to preparation. The somata are large (up to 1 mm in diameter) and are physically very accessible for complex neurophysiological manipulations. Several microelectrodes can be positioned in or around the soma or initial axon segment, and fiberoptic light pipes can even be positioned in order to monitor optical changes within the neuron.

Aplysia giant neurons have been the subject of many neurophysiological studies (19,26,37, 68,97); therefore, background data are available concerning the known Ca^{2+}, Na^{+}, and K^{+} conductances of these cells. A very important reason for the use of this preparation in the

study of slow currents is that the giant cells are very stable *in vivo* and can remain viable for greater than 12 hr. Long-term stability and viability was crucial for this type of study because of the extended periods of time necessary to obtain SOC tail data with drugs. Often, 2 hr are required for each concentration of drug and to obtain responses across a wide concentration range requires that an experiment continue for up to 10–16 hr. In most cases, the giant cell preparations are able to sustain this long-term viability.

Tail Analysis

Plotting the tail currents on semilogarithmic graph paper revealed that SOC tail currents appeared to be made up of at least two exponential decay processes. A more rigorous method of analysis was developed in order to determine the kinetics and amplitudes of tail currents more accurately. A compartmental analysis program was modified to perform an automatic curve peel (98) on tail current data. Figure 3 shows an example of SOC and tail current obtained in control solutions and with added barbiturate, in this case 100 μM secobarbital. The raw data are shown in panel A, whereas panel B shows semilogarithmic plots of the tail currents and the best-fit curves obtained from the analysis program (solid lines).

The analysis program relies on the following assumptions: (a) the process under study is made up of multiple exponential decay components; and (b) the individual decay components are of reasonably different kinetics. A subtle requirement of the program is that data must be collected in such a fashion that there are enough points to represent each component of decay adequately, i.e., relatively more points are needed during the early portions of tail than the late portions of tail. This was usually accomplished by collecting the first points in a tail at twice the rate (0.5 Hz) of the second half (0.25 Hz).

The method of the tail analysis was similar to a manual "peel": (a) the slowest component of decay was determined; (b) the contribution of the slow component was removed from fast components by subtraction; and (c) the next slower component of decay was determined. The process was repeated until there were no more points.

More sophisticated methods than peeling are available for the determination of the parameters describing a multicomponent exponential decay process, such as nonlinear least-squares fitting routines. However, when these methods were applied to the analysis of tail currents, it was found that the results were not appreciably different from those obtained with the peeling routine. Therefore, the advantages of ease and rapidity of peeling were chosen at the expense of a small decrement in the accuracy of the estimates for the parameters, as compared with least-squares fitting routines.

The results of tail analysis most often yielded two components with half-lives of ~10 and ~60 sec. However, in some cases, three components were described. In these cases, it was found that the tails could be reasonably well fit with a two-component tail. In all cases in which an equally good fit would be obtained with models of differing complexity, the least complex model (that with fewest components) was assumed.

K^+ Sensitivity

The rate of rise of SOC and the reversal potential for SOC tails have previously been shown to depend on the level of extracellular K^+ (29). Using tail-current analysis, we tested the sensitivity of both of the components of tail current and found that each component was approximately equally affected by changes in $[K^+]_o$. Figure 10 shows tail currents obtained by depolarizing from a holding potential of −50 mV to −35 mV for 60 sec in artificial seawater (ASW) with three different levels of $[K^+]_o$. Panel A is a linear plot of the tail currents; panel B shows the tail currents on a semilog plot. In the semilog plot, the currents are paralleled over the entire time course of the tail. This indicates that the major difference between the currents is one of *magnitude,* as one would expect with the change in driving force produced by altering the potassium equilibrium potential.

The tail currents can be converted to conductance measurements based on these assumptions:

1. Tail currents are the result of K^+ conductance changes according to the following rearrangement of Ohm's law:

$$I_K = g_K(E_K - E_m), \qquad \text{(Eq. 1)}$$

where I_K is the potassium current, g_K is the potassium conductance, E_K is the potassium equilibrium potential, and E_m is the membrane potential.

2. E_K was calculated based on the Nernst equation:

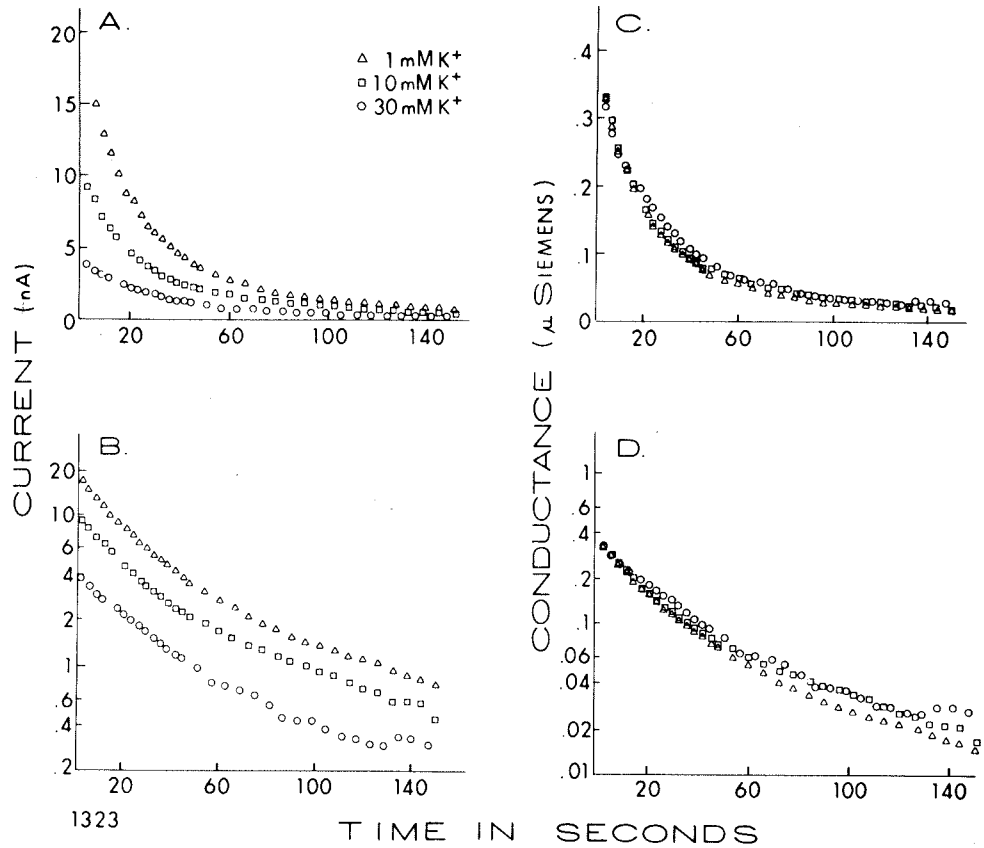

FIG. 10. Sensitivity of SOC tail currents to extracellular potassium levels. **A**: Linear plots of tail currents obtained with different levels of extracellular potassium. **B**: Semilog plots of the data in **A**. **C**: Tail currents from **A** converted to tail conductances based on the assumptions stated in test, linear plot. **D**: Semilog plots of the data in **C**. Stimulus was a 60-sec depolarization to −30 mV from a holding potential of −50 mV. From Huguenard et al., ref. 54a, with permission.

$$E_K = \frac{RT}{Fz} \times \text{Ln}\left(\frac{[K^+]_o}{[K^+]_i}\right) \qquad \text{(Eq. 2)}$$

where R is the universal gas constant, T is the temperature in °K, F is the Faraday constant, and z is the valence of the ion, in this case, 1.

3. Intracellular $[K^+]$ was assumed to be 158 mM (measured as described in the following section).

These conductance curves are plotted in panel C on a linear scale and again in panel D on a semilog scale. The curves largely overlap each other, verifying the assumption that tail currents are primarily caused by changes in K^+ conductance.

Tail reversal experiments were performed in order to verify that SOC tails were strictly dependent on the potassium equilibrium potential. These experiments proved fairly difficult to perform as a result of slow changes in other currents which occurred at very hyperpolarized potentials. However, in some cases we were able to reverse the tail currents, and as previously shown (29), the reversal potential was found to depend on the extracellular level of potassium.

Extracellular Potassium Accumulation

In two experiments, a K^+-sensitive microelectrode was positioned near the soma of the giant neuron R2 to examine changes in extracellular K^+-induced during SOC. Figure 11 shows that the results of one of these experiments. In this case, the K^+-sensitive electrode was placed so that it was actually touching the membrane of neuron R2. The extracellular K^+ levels follow the kinetics of SOC activation and tail inactivation reasonably well.

At the end of the experiment, the K^+-sensi-

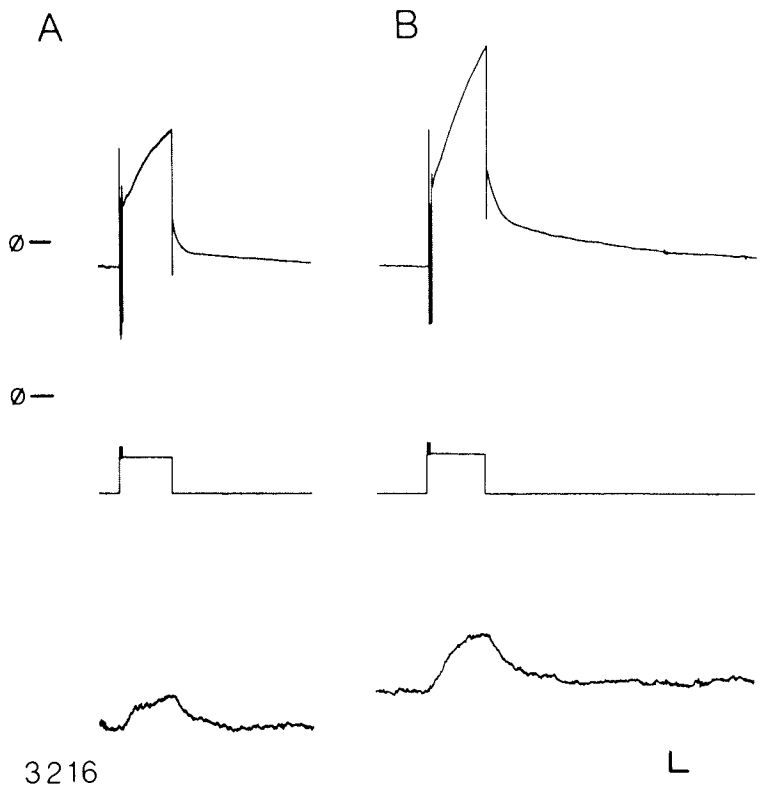

FIG. 11. Extracellular potassium accumulation during slow outward current (SOC) and tail currents; effects of pentobarbital. *Upper traces:* voltage clamp currents; *middle traces:* voltage levels; *lower traces:* potential measured at the potassium sensitive electrode. **A:** Control. **B:** Pentobarbital, 100 μM. Calibration: vertical 5 nA, 10 mV, and 5 mM K^+; horizontal 20 sec.

tive electrode was put into the neuron in order to obtain an estimate of $[K^+]_i$. According to the calibration obtained with different levels of K^+ in ASW, $[K^+]_i$ was 158 mM.

Sensitivity of Tail Currents to Alterations of Other Ions

The results of sodium substitution experiments were somewhat variable. In general, replacement of $[Na^+]_o$ by equiosmolar concentrations of sucrose or *bis*-tris-propane markedly reduced the SOC and tail currents. The tail currents were usually reduced to such levels that analysis became impractical because of the decreased signal to noise ratio. However, in every case, the addition of pentobarbital to the perfusate was able to reverse the inhibition. Although the sensitivity of SOC or Cl^- was not specifically studied, the sucrose substitution experiments resulted in removal of most of the extracellular Cl^-, and as mentioned above, SOC persisted in these experiments, especially with barbiturate added.

Removal of Ca^{2+} from the ASW resulted in depression of SOC and tail current. To reduce further the extracellular Ca^{2+} to very low levels, the specific calcium chelator EGTA (2 mM) was added to 0 Ca^{2+} ASW. Surprisingly, in the presence of EGTA, the SOC and tail current were restored to near control levels. This may be caused by the removal of membrane screening charges (35), which would result in a stronger net depolarization of the membrane. Moderate doses of pentobarbital were also able to restore, and usually exceed, control SOC and tail current levels.

Figure 12 shows the tail currents from a Ca^{2+} experiment. As can be seen, removal of extracellular Ca^{2+} caused a marked decrease in the amplitude of the tail current, with any slow component becoming indistinguishable from noise. The addition of 2 mM EGTA restored the tail currents towards control levels, and the addition

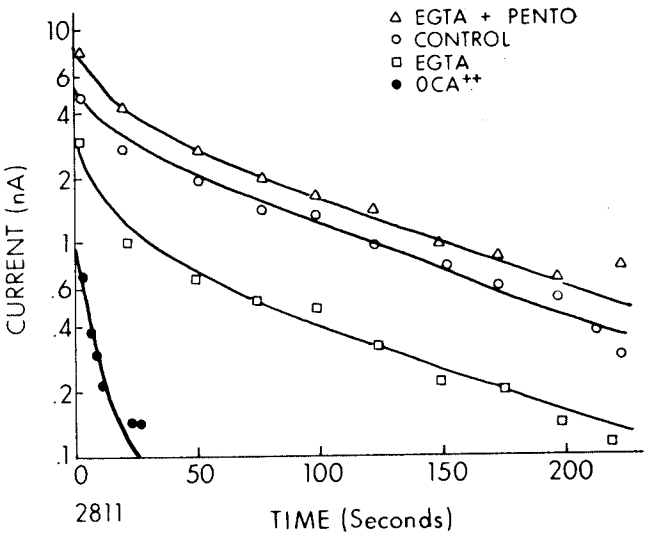

FIG. 12. Effect of removal of extracellular calcium on tail currents; effects of pentobarbital. Stimulus, 60-sec depolarization to −32 from a holding potential of −50 mV. EGTA, 2 mM; pentobarbital, 100 μM.

of 100 μM pentobarbital further increased the amplitude of tail current.

Lewis and Wilson (68) have shown that the initial portion of adaptation (5 sec) in *Aplysia* giant cells is caused by Ca^{2+} entry which leads to activation of a potassium current. As shown in Fig. 12, removal of extracellular Ca^{2+} does not block tail currents (nor does it block SOC). Adaptation responses were obtained in this situation to verify that late adaptation does occur in the absence of Ca^{2+}. As shown in Fig. 13, slow adaptation does persist (although at a different level) in the absence of extracellular Ca^{2+}, and pentobarbital does enhance the slow adaptation.

It should be pointed out here that the tail currents obtained in these neurons after a brief (2 sec) burst of action potentials are qualitatively quite similar to SOC tail currents. Both types of tail currents can be represented by multicom-

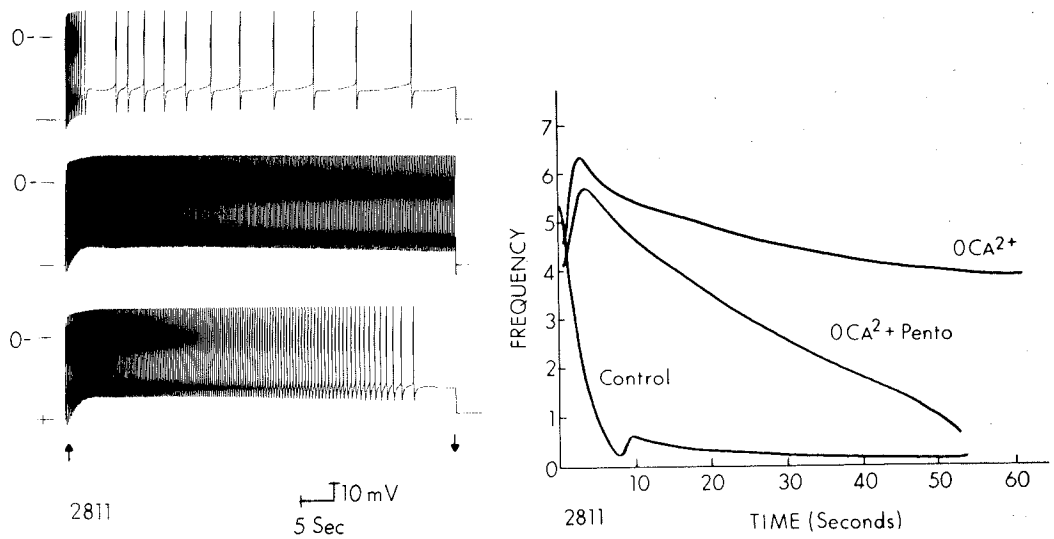

FIG. 13. Effect of removal of extracellular calcium on adaptation; effects of added pentobarbital. **A:** Adaptation responses in control, *upper trace;* OCa^{2+}, *middle trace;* and OCa^{2+} with pentobarbital, *lower trace.* **B:** Spike frequency plots of the data in part **A.** Stimulus, 60-sec constant current depolarization of 25 nA from a holding potential of −50 mV; pentobarbital, 100 μM.

ponent exponential decay processes with similar kinetics. However, there are differences between the two currents. The tail current after a brief burst of spikes (postspike current, PSC) is not affected by concentrations of barbiturates that cause a marked enhancement of SOC tail currents (34). The PSC is totally eliminated by the removal of extracellular Ca^{2+}, but the SOC tail current does not require extracellular Ca^{2+} (see Fig. 12). Intracellular injection of the Ca^{2+} chelator, EGTA, resulted in blockade of PSC at concentrations that did not affect SOC or tail current. However, much higher concentrations of EGTA did diminish both SOC and tail current. Both the Ca^{2+}-dependent light response (14) and the response to iontophoretic injection of Ca^{2+} were unaffected by 100 μM pentobarbital. Therefore, although SOC is somewhat sensitive to Ca^{2+}, it does not seem to be dependent on Ca^{2+} entry. In addition, it appears that barbiturates are *not* exerting their effect by producing an increased sensitivity to the intracellular level of Ca^{2+}.

Kinetic Model of Slow Outward Current

The existence of *two* components of outward tail current along with the selective enhancement of one of the components by barbiturates led us to develop several models that might explain these phenomena.

We originally hypothesized that SOC may result from the activation of two different types of potassium channels. However, there was much evidence to indicate that the two components of tail current were not independent. Any manipulation that resulted in a diminution of SOC and tail current could be reversed by the addition of barbiturate, and the barbiturate-induced restoration normally affected *both* components of tail. For example, although removal of extracellular Ca^{2+} or the addition of Ca^{2+} channel blockers La^{3+} or Co^{2+} resulted in a marked decrease in SOC and the amplitude of both tail components, barbiturate restored all of these parameters to at least control levels. We were unable to find any one agent that would selectively block one of the components. Therefore, it appeared that SOC could not be easily explained by the existence of two conductance mechanisms, one of which is enhanced by barbiturates. A more reasonable mechanism seemed to be that there were several regulatory factors affecting one conductance mechanism.

Several sequential models were developed to explain how alterations in one type of channel could result in tail current kinetics that resembled two types of channel. These sequential models involved such events as the activation of a channel by depolarization of the membrane, followed by binding of the channel by Ca^{2+}, which would further activate the channel. Another possibility was that Ca^{2+} was an enabling agent for the ionic channels underlying SOC. The enabling action of Ca^{2+} allowed membrane depolarization to activate the channels. Some of these models were quite complex; however, none of them could easily explain SOC and the enhancement produced by barbiturates. In each case, complex alterations by barbiturates of more than one parameter of the model were necessary to obtain predicted curves similar to those obtained in actual experiments.

Two factors led us to develop a different type of model. First, an early study by Pallotta et al. (78) of Ca^{2+}-activated K^+ channels in cultured rat myotubules demonstrated that these channels were regulated by two factors: intracellular level of Ca^{2+}, and membrane potential. Because SOC is caused by a K^+ conductance and is somewhat dependent on Ca^{2+}, we hypothesized that a Ca^{2+} activated K^+ mechanism such as that elucidated by Pallotta might underlie SOC. Second, we found evidence in the literature (5,49,84) that there may be a voltage-sensitive intracellular release of Ca^{2+} in neurons and other cells, similar to the release of Ca^{2+} from sarcoplasmic reticulum in muscle (95). We hypothesized that the combination of these two mechanisms (Ca^{2+}-activated K^+ conductance and depolarization-activated Ca^{2+} release) would explain SOC, and that barbiturate alteration of one of these mechanisms would explain the changes in SOC produced by barbiturates.

To test the model, we developed a mathematical relationship describing all of the parameters of the model. The simplest basis of the model is the potassium channel itself;

$$CH_{closed} \underset{KC}{\overset{KO}{\rightleftharpoons}} CH_{open} \qquad \text{(Eq. 3)}$$

In this simple model, KC, the channel-closing rate, is constant. KO, the channel-opening rate, is a function of membrane potential and intracellular Ca^{2+}. Ca^{2+} is an agonist which increases KO according to the Michaelis-Menton relationship:

$$KO = \frac{KO_{max}}{(Km/[Ca]) + 1} \qquad \text{(Eq. 4)}$$

However, membrane potential also affects this

relationship such that hyperpolarization is antagonistic to the effects of Ca^{2+}. A competitive antagonist effectively increases the Km for a reaction. With this in mind, we developed the following relationship for the value of Km in equation 4:

$$Km = Km_{min}\,(1 + e^{((Kv-V)/SF)}) \qquad \text{(Eq. 5)}$$

Km is the apparent Km, Km_{min} is the minimum Km, V is the membrane potential, Kv is the membrane potential at which Km is 2 × Km_{min}, and SF is a factor that determines the steepness of the relationship between voltage and apparent Km. As V becomes hyperpolarized, the apparent Km becomes larger, so that a higher concentration of Ca^{2+} is necessary to attain the same channel-opening rate. A three-dimensional representation of this relationship at equilibrium can be seen in Fig. 14. The parameters that were used to generate Fig. 14 are as follows: KO_{max} = 10/sec; KC = .05/sec; Km_{min} = 50 μM, SF (slope factor) = 13; and Kv = 0 mV. As can be seen, Ca^{2+} becomes less effective at opening channels with more negative (hyperpolarized) potentials. In fact, there is further evidence that this is exactly the character of these channels. Compare this figure with Fig. 8D in Barrett et al. (13). Although the vertical axis in that figure indicates percentage of time open, this could be easily converted to percentage of channels open by multiplying this value by the total number of channels. Thus, the description of the channels in this model closely resembles the actual voltage and calcium sensitivity of the channels studied in isolation.

Thus far, we have described the channels that may underlie slow outward current. To understand how this might work, we must discuss part 2 of the model, which states that there is a voltage-dependent release of Ca^{2+} inside the neuron. The control of Ca^{2+} within this system can be described by the following equation:

$$Ca_{bound} \underset{KU}{\overset{KR}{\rightleftharpoons}} Ca_{free} \qquad \text{(Eq. 6)}$$

Ca_{bound} is the releasable Ca^{2+} which is available to interact with the K^+ channels, KU is the rate of Ca^{2+} uptake, a constant, and KR is the rate of Ca^{2+} release, which is a sigmoidal function of membrane potential according to the following relationship:

$$KR = \frac{KR_{max}}{1 + e^{(Kvr-V/SF2)}} \qquad \text{(Eq. 7)}$$

KR_{max} is the maximum rate of Ca^{2+} release, Kvr is the membrane potential at which the Ca^{2+} release is half maximal, V is the membrane potential, and SF2 is the scaling factor that determines the steepness of the relationship between voltage and the rate of Ca^{2+} release.

Based on these mathematical relationships,

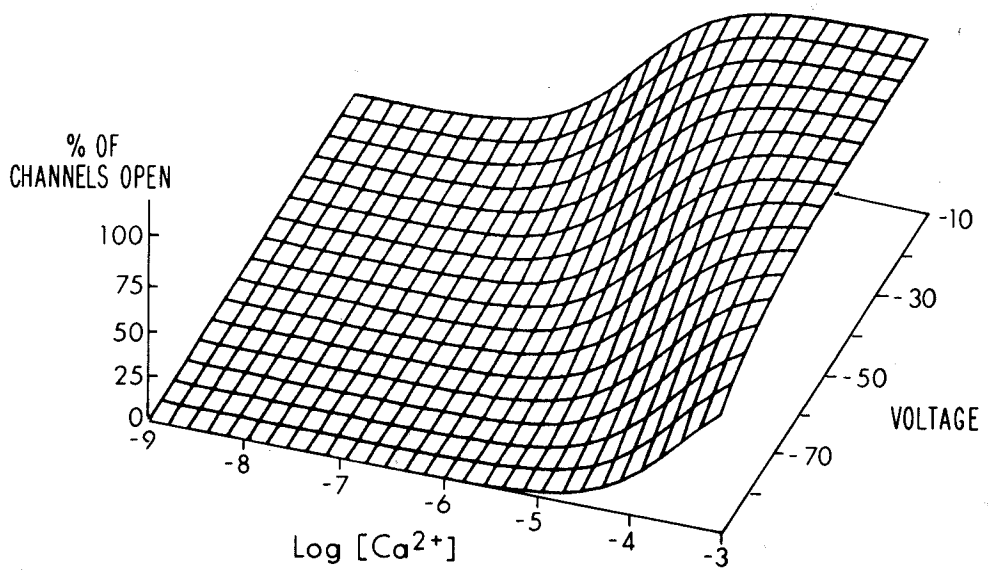

FIG. 14. Three-dimensional representation of one aspect of the model, the channels underlying slow outward current. The dependence on calcium levels and membrane potential is indicated. Either increased free intracellular calcium or depolarization of the membrane results in a greater percentage of open channels.

we were able to describe an equilibrium level of Ca^{2+} and the equilibrium number of channels open at any one membrane potential and to study the time-dependent changes in the current (number of channels open). The effects of perturbation of the system from equilibrium were predicted using standard kinetic procedures. An iterative procedure was used in which the voltage-induced change in Ca^{2+} was calculated for a short time interval; the resultant change in the channel opening rate and the number of channels opened during that interval could then be determined. This iteration was repeated for the duration of the stimulated depolarization. In this way, we could predict the time course of both the change in intracellular Ca^{2+} and the change in number of channels open. Finally, we predicted that barbiturates altered the voltage sensitive calcium release, so that depolarization became more effective at releasing calcium. To test this theory, we studied the effects of changes in Kvr (in equation 7) on the voltage- and time-dependent kinetics of intracellular Ca^{2+} and the number of channels open.

Figure 15 is a three-dimensional representation of what the time-dependent onset of SOC might look like with various concentrations of barbiturate. The time axis represents the time of depolarization to −30 mV from a holding potential of −50 mV. The number of channels open at time = 0 is equivalent to the number of channels that are open at the holding potential. With increasing duration of depolarization, there is a slow increase in the number of channels open. The effect of increased barbiturate concentration are twofold: first, there is an increase in the rate of development of open channels with depolarization; second, with high concentrations of barbiturate, there is an increase in the number of channels open at the holding potential. Both of these effects predicted by the model are quite evident in barbiturate experiments. Increasing concentrations of barbiturates do result in an increased rate of SOC (channel opening), and at higher doses there is a large increase in outward current at the holding potential.

We also looked at the predictions that the model makes for tail currents and the changes produced by barbiturates. Figure 16A shows the tail currents that are predicted from the model with changes in Kvr (the voltage at which the half-maximal rate of Ca^{2+} release occurs). Curves 1 through 4 are the predicted tail currents after a 60-sec depolarization to −30 mV from a holding potential of −50 mV. Curve 4 corresponds to a Kvr of 0 mV; curve 3 to −5

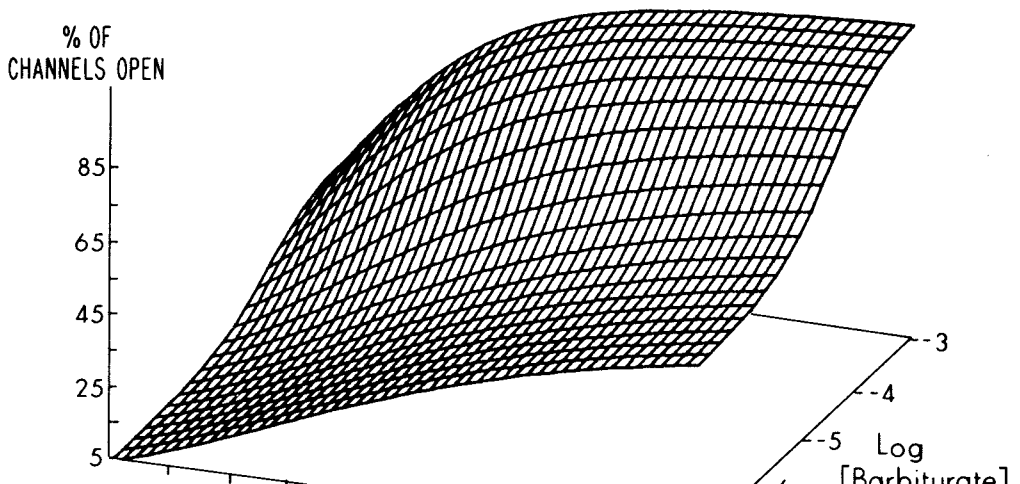

FIG. 15. Illustration of the time dependence of channel opening and alterations produced by the addition of barbiturate. Time in this figure indicates the duration of depolarization to −30 mV from a holding potential of −50 mV. With depolarization, intracellular free calcium slowly increases toward a new steady state; this underlies the slow time course of the slow outward current. In this model, barbiturates are thought to enhance the voltage-dependent increase in intracellular calcium and the resultant activation of potassium channels.

mV; curve 2 to −10 mV; and curve 1 corresponds to −15 mV. The result of making depolarization more effective in releasing Ca^{2+} is an increase in tail amplitude, with a somewhat selective enhancement of the amplitude of the slow component of tail. Part B of Fig. 16 shows the results of an actual barbiturate experiment (in this case, secobarbital) for comparison purposes. Although the actual currents in Fig. 16C are somewhat more noisy than the predicted currents (as a result of small spontaneous synaptic events), the model is quite capable of describing the effects of barbiturates qualitatively.

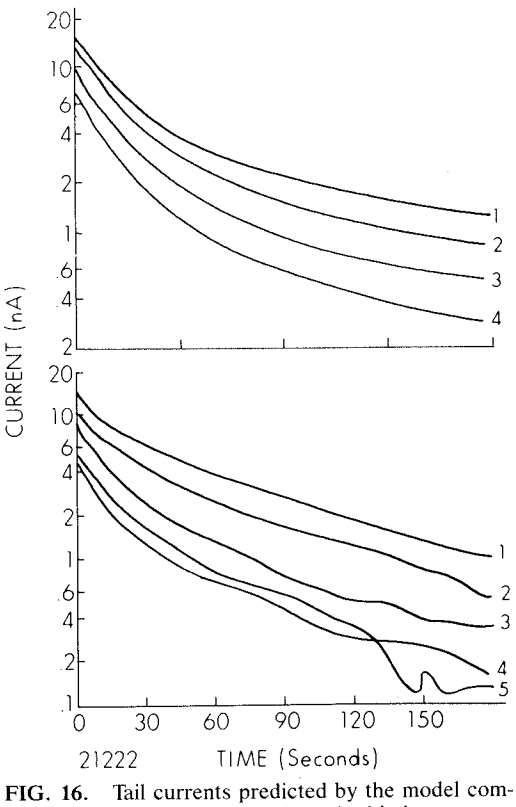

FIG. 16. Tail currents predicted by the model compared with results of an actual secobarbital concentration-response experiment. **A:** Tail currents predicted as a result of changing the voltage sensitivity of calcium release. Curves 1–4 represent the effects of decreasing the voltage-sensitive calcium release (i.e., depolarization becomes less effective in releasing calcium). **B:** Tail currents from a secobarbital concentration-response experiment: 4, control; 3, 25 μM secobarbital; 2, 50 μM secobarbital; 1, 100 μM secobarbital; 5, wash. Thus, the effects of increasing concentrations of barbiturates can be paralleled in the model by shifts in the voltage sensitivity of calcium release. Stimulus, 60-sec depolarization to −34 from a holding potential of −50 mV.

Therefore, we have a model that can explain not only the two components of tail current, but the alterations in SOC and tail current produced by barbiturate as well. Obviously, this is only one of several models or derivations of this model that can explain the data. In general, this type of current can be explained by the voltage-dependent levels of some factor; this factor affects the voltage sensitivity of the ionic channels underlying the current.

ACKNOWLEDGMENTS

We would like to thank Drs. Robert Zucker, Richard Kramer, William Adams, and Irwin Levitan for their valuable advice and assistance and for allowing us to refer to their most recent work in this review.

REFERENCES

1. Adams, W. B., and Levitan, I. B. (1981): Ionic dependence and charge carriers of the currents underlying bursting in *Aplysia* neuron R15. *Soc. Neurosci. Abstr.*, 7:863.
2. Adams, W. B., and Levitan, I. B. (1982): Origin of the depolarizing after-potential in *Aplysia* cell R15. *Soc. Neurosci. Abstr.*, 8:126.
3. Adams, W. B., Parnas, I., and Levitan, I. B. (1980): Mechanism of long lasting inhibition in *Aplysia* neuron R15. *J. Neurophysiol.*, 44:1148–1160, 1980.
4. Ahmed, Z., and Connor, J. A. (1979): Measurement of calcium influx under voltage clamp in molluscan neurones using the metallochronic dye Arsenazo III. *J. Physiol (Lond.)*, 286:61–82.
5. Akaike, A. M., Brown, A. M., Dahl, G., Highashi, H., Isenberg, G., Tsuda, Y., and Yatani, A. (1983): Voltage-dependent activation of potassium current in *Helix* neurones by endogenous cellular calcium. *J. Physiol.*, 334:309–324.
6. Alving, B. O. (1968): Spontaneous activity in isolated somata of *Aplysia* pacemaker neurons. *J. Gen. Physiol.*, 51:29–45.
7. Anderson, W. W., and Barker, D. L. (1981): Synaptic mechanisms that generate network oscillations in the absence of discrete postsynaptic potentials. *J. Exp. Zool.*, 216:187–191.
8. Anderson, W. W., Wilson, W. A., and Lewis, D. V. (1984): Dopamine enhancement of a spike-evoked current in the *Aplysia* bursting neuron R15. *Neurosci. Abstr.* 10:204.
9. Ascher, P. (1972): Inhibitory and excitatory effects of dopamine on *Aplysia* neurons. *J. Physiol. (Lond.)*, 225:173–209.
10. Baldissera, F., and Gustafsson, B. (1971): Regulation of repetitive firing in motoneurones by the afterhyperpolarization conductance. *Brain Res.*, 30:431–434.
11. Barker, J. L., Ifshin, M. S., and Gainer, H. (1975): Studies on bursting pacemaker potential

activity in molluscan neurons. III. Effects of hormones. *Brain Res.*, 84:501–515.
12. Barker, J. L., and Smith, T. G., Jr. (1978): Electrophysiological studies of molluscan neurons generating bursting pacemaker potential activity. In: *Abnormal Neuronal Discharges*, edited by N. Chalazonitis and M. Buisson, pp. 359–387. Raven Press, New York.
13. Barrett, J. N., Magleby, K. L., and Pallotta, B. S. (1982): Properties of single calcium-activated potassium channels in cultured rat muscle. *J. Physiol.*, 331:211–230.
14. Baur, P. S., Jr., Brown, A. M., Rogers, T. D., and Brower, M. E. (1977): Lipochondria and the light response of *Aplysia* giant neurons. *J. Neurobiol.*, 8:19–42.
15. Baylor, D. A., and Nichols, J. G. (1969): After-effects of nerve impulses on signalling in the central nervous system of the leech. *J. Physiol.*, 203:571–589.
16. Benardo, L. S., and Prince, D. A. (1982): Dopamine action on hippocampal pyramidal cells. *J. Neurosci.*, 2:415–423.
17. Brown, A. M., and Brown, H. M. (1973): Light response of a giant *Aplysia* neuron. *J. Gen. Physiol.*, 62:239–254.
18. Bragdon, A. C., and Wilson, W. A. (1982): CA1 pyramidal cells exhibit spike frequency adaptation and a slow outward current. *Soc. Neurosci, Abstr.*, 287.16.
19. Brodwick, M. S., and Junge, D. (1972): Post-stimulus hyperpolarization and slow potassium conductance increase in *Aplysia* giant neurons. *J. Physiol.*, 223:549–570.
20. Carnevale, N. T. (1973): Voltage clamp analysis of the slow oscillations in bursting neurons reveals two underlying current components. PhD Dissertation, Duke University, Durham, N.C.
21. Carnevale, N. T., and Wachtel, H. (1980): Two reciprocating current components underlying slow oscillations in *Aplysia* bursting neurons. *Brain Res. Rev.*, 2:45–68.
22. Carpenter, D. O., and Alving, B. O. (1968): A contribution of an electrogenic Na^+ pump to membrane potential in *Aplysia* neurons. *J. Gen. Physiol.*, 52:1–21.
23. Carpenter, D., and Gunn, R. (1970): The dependence of pacemaker discharge of *Aplysia* neurons on Na^+ and Ca^{++}. *J. Cell. Physiol.*, 75: 121–128.
24. Chen, C. F., von Baumgarten, R., and Takeda, R. (1971): Pacemaker properties of completely isolated neurons in *Aplysia californica*. *Nature New Biol.*, 233:27–29.
25. Colding-Jorgensen, M. (1977): Impulse dependent adaptation in *Helix Pomatia* neurones: Effect of the impulse on the firing pattern. *Acta. Physiol. Scand.*, 101:369–381.
26. Colmers, W. F., Lewis, D. V., Jr., and Wilson, W. A. (1982): Cs^+ loading reveals Na^+-dependent persistent inward current and negative slope resistance region in *Aplysia* giant neurons. *J. Neurophys.*, 48:1191–1200.
27. Colquhoun, D., Neher, E., Reuter, H., and Stevens, C. F. (1981): Inward current channels activated by intracellular Ca in cardiac cells. *Nature*, 294:752–754.
28. Connor, J. A. (1979): Calcium current in molluscan neurones: Measurement under conditions which maximize its visibility. *J. Physiol. (Lond.)*, 286:41–60.
29. Cote, I. L., Zbicz, K. L., and Wilson, W. A. (1978): Barbiturate-induced slow outward currents in *Aplysia* neurones. *Nature*, 274:594–596.
30. Dipolo, R., Requena, J., Brinley, F. J., Jr., Mullins, L. J., Scarpa, A., and Tiffert, T. (1976): Ionized calcium concentrations in squid axons. *J. Gen. Physiol.*, 67:433–467.
31. Eckert, R., and Lux, H. D. (1976): A voltage-sensitive persistent calcium conductance in neuronal somata of *Helix*. *J. Physiol.*, 254:129–151.
32. Eckert, R., and Tillotson, D. (1978): Potassium activation associated with intraneuronal free calcium. *Science*, 200:437–439.
33. Eckert, R., and Tillotson, D. L. (1981): Calcium-mediated inactivation of the calcium conductance in caesium loaded giant neurones of *Aplysia californica*. *J. Physiol. (Lond.)*, 314:265–280.
34. Evans, G. J., Huguenard, J. R., Wilson, W. A., and Lewis, D. V. (1982): Enhancement of slow outward current by pentobarbital is independent of Ca^{++} entry. *Soc. Neurosci. Abstr.*, 194.3.
35. Frankenhaeuser, B., and Hodgkin, A. L. (1957): The action of calcium on the electrical properties of squid axons. *J. Physiol.*, 137:218.
36. Gainer, H. (1972): Electrophysiological behavior of an endogenously active neurosecretory cell. *Brain. Res.*, 39:403–418.
37. Geduldig, D., and Junge, D. (1968): Sodium and calcium components of action potentials in the *Aplysia* giant neurones. *J. Physiol.*, 199:347–365.
38. Gola, M. (1974): Neurones a ondes-salves des mollusques. Variations cycliques lentes des conductances ioniques. *Eur. J. Physiol.*, 352:17–36, 1974.
39. Gorman, A. L. F., and Hermann, A. (1979): Internal effects of divalent cations on potassium permeability in molluscan neurons. *J. Physiol. (Lond.)*, 296:393–410.
40. Gorman, A. L. F., Hermann, A., and Thomas, A. V. (1982): Ionic requirements for membrane oscillations and their dependence on calcium concentration in a molluscan pace-maker neurone. *J. Physiol. (Lond.)*, 327:185–217.
41. Gorman, A. L. F., and Thomas, M. V. (1978): Changes in the intracellular concentration of free calcium ions in a pace-maker neurone measured with the metallochromic indicator dye Arsenazo III. *J. Physiol. (Lond.)*, 275:357–376.
42. Gorman, A. L. F., and Thomas, M. V. (1980a): Intracellular calcium accumulation during depolarization in a molluscan neurone. *J. Physiol. (Lond.)*, 308:259–285.
43. Gorman, A. L. F., and Thomas, M. V. (1980b): Potassium conductance and internal calcium accumulation in a molluscan neurone. *J. Physiol. (Lond.)*, 308:287–313.
44. Gospe, S. M., Jr. (1983): Minireview: Studies of

dopamine pharmacology in molluscs. *Life Sci.*, 33:1945–1957.
45. Gospe, S. M., Jr., and Wilson, W. A., Jr. (1980): Dopamine inhibits burst-firing of neurosecretory cell R15 in *Aplysia californica:* Establishment of a dose response relationship. *J. Pharmacol. Exp. Ther.*, 214:112–118.
46. Gospe, S. M., Jr., and Wilson, W. A., Jr. (1981): Pharmacological studies of a novel dopamine-sensitive receptor mediating burst-firing inhibition of neurosecretory cell R15 in *Aplysia californica. J. Pharmacol. Exp. Ther.*, 216:368–377.
47. Gulrajani, R. M., and Roberge, F. A. (1978): Possible mechanisms underlying bursting pacemaker discharges in invertebrate neurons. *Fed. Proc.*, 37:2146–2152.
48. Hagawara, S., and Byerly, L. (1981): Calcium channel. *Annu. Rev. Neurosci.*, 4:69–125.
49. Henkart, M. P., and Nelson, P. G. (1979): Evidence for an intracellular calcium store releasable by surface stimuli in fibroblasts (L cells). *J. Gen. Phys.*, 73:655–673.
50. Hermann, A., and Gorman, A. L. F. (1979): External and internal effects of tetraethylammonium on voltage-dependent and Ca-dependent K^+ currents components in molluscan pacemaker neurons. *Neurosci. Lett.*, 12:87–92.
51. Heyer, C. B., and Lux, H. D. (1976): Control of the delayed outward potassium currents in the bursting pacemaker neurons of the snail, *Helix pomatia. J. Physiol. (Lond.)*, 262:349–382.
52. Hille, B., Woodhull, A. M., and Shapiro, E. I. (1975): Negative surface charge near sodium channels of nerve: Divalent ions, monovalent ions and pH. *Philos. Trans. R. Soc. (Lond.) B* 270:301–318.
53. Hofmeier, G., and Lux, H. D. (1981): The time courses of intracellular free calcium and related electrical effects after injection of $CaCl_2$ into neurons of the snail, *Helix pomatia. Pflugers Arch.*, 391:242–251.
54. Huguenard, J. R., and Wilson, W. A. (1985): Suppression of repetitive firing of neurons by diphenylbarbituric acid. *J. Pharmacol. Exp. Ther.*, 232:228–231.
54a. Huguenard, J. R., Zbicz, K. L., Lewis, D. V., Evans, G. J., and Wilson, W. A. (1985): The ionic mechanism of the slow outward current in *Aplysia* neurons. *J. Neurophysiol.*, 54:449–461.
55. Ito, M., and Oshima, T. (1962): Temporal summation of after-hyperpolarisation following a motoneurone spike. *Nature*, 195:910–911.
56. Johnston, D. (1976): Voltage clamp reveals basis for calcium regulation of bursting pacemaker potentials in *Aplysia* neurons. *Brain Res.*, 107:418–423.
57. Johnston, D. (1980): Voltage, temperature and ionic dependence of the slow outward current in *Aplysia* burst-firing neurones. *J. Physiol. (Lond.)*, 289:145–157.
58. Junge, D., and Stephens, C. L. (1973): Cyclic variation of potassium conductance in a burst-generating neurone in *Aplysia. J. Physiol. (Lond.)*, 235:155–181.
59. Kernell, D. (1965): The adaptation and the relation between discharge frequency and current strength of cat lumbosacral motoneurones stimulated by long-lasting injected currents. *Acta Physiol. Scand.*, 65:65–73.
60. Kernell, D., and Monster, A. W. (1982): Time course and properties of late adaptation in spinal motoneurons of the cat. *Exp. Brain Res.*, 46:191–196.
61. Kramer, R. H. (1984): The ionic mechanism of bursting pacemaker activity in *Aplysia* neurons. Ph.D. Dissertation. University of California at Berkeley.
62. Kramer, R. H., and Zucker, R. S. (1983): Inactivation of persistent inward current mediates post-burst hyperpolarization in *Aplysia* bursting pacemaker cells. *Soc. Neurosci. Abstr.*, 9:510.
63. Krnjevic, K., and Lisiewicz, A. (1972): Injections of calcium ions into spinal motoneurons. *J. Physiol. (Lond.)*, 225:363–390.
64. Krnjevic, K., Puil, E., and Werman, R. (1978): EGTA and motoneuron afterpotentials. *J. Physiol. (Lond.)*, 275:199–223.
65. Levitan, I. B., Harmon, A. J., and Adams, W. B. (1979): Synaptic and hormonal modulation of a neuronal oscillator: A search for molecular mechanisms. *J. Exp. Biol.*, 81:131–151.
66. Lewis, D. V. (1984): Spike aftercurrents in R15 of *Aplysia*. Their relationship to slow inward current and calcium influx. *J. Neurophysiol.*, 51: 403–419.
67. Lewis, D. V., Evans, G. B., and Wilson, W. A. (1984): Dopamine reduces slow outward current and calcium influx in burst firing neuron R15 of *Aplysia. J. Neurosci.*, 4:3014–3020.
68. Lewis, D. V., and Wilson, W. A. (1982): Calcium influx and poststimulus current during early adaptation in *Aplysia* giant neurons. *J. Neurophysiol.*, 48:202–216.
69. Lux, H. D., and Heyer, C. B. (1979): A new electrogenic calcium-potassium system. In: *The Neurosciences Fourth Study Program*, edited by F. O. Schmitt and F. G. Worden, pp. 601–615. M.I.T. Press, Cambridge, Mass.
70. Maruyama, Y., and Peterson, O. H. (1982): Single channel currents in isolated patches of plasma membrane from basal surface of pancreatic acini. *Nature*, 299:159–161.
71. Mayeri, E., Brownell, P., Branton, W. D., and Simon, S. B. (1979): Multiple, prolonged actions of neuroendocrine bag cells on neurons in *Aplysia*. I. Effects on bursting pacemaker neurons. *J. Neurophysiol.*, 42:1165–1184.
72. Meech, R. W. (1972): Intracellular calcium injection causes increased potassium conductance in *Aplysia* nerve cells. *Comp. Biochem. Physiol.*, 42A:493–499.
73. Meech, R. W. (1974): Calcium influx induces a post tetanic hyperpolarization in *Aplysia* neurones. *Comp. Biochem. Physiol.*, A48:387–395.
74. Meech, R. W. (1974): The sensitivity of *Helix aspersa* neurones to injected calcium ions. *J. Physiol. (Lond.)*, 237:259–277.
75. Meech, R. W. (1979): Membrane potential oscillations in molluscan "burster" neurones. *J. Exp. Biol.*, 81:93–112.
76. Meech, R. W., and Standen, N. B. (1975): Potassium activation in *Helix Aspersa* neurones under voltage clamp. A component mediated by calcium influx. *J. Physiol. (Lond.)*, 249:211–239.

77. Moulins, M., and Cournil, I. (1982): All-or-none control of the bursting properties of the pacemaker neurons of the lobster pyloric pattern generator. *J. Neurobiol.*, 13:447–458.
78. Pallotta, B. S., Magleby, K. L., and Barrett, J. N. (1981): Single channel recordings of Ca^{2+} activated K^+ currents in rat muscle cell culture. *Nature*, 293:471–474.
79. Parnas, I., Armstrong, D., and Strumwasser, F. (1974): Prolonged excitatory and inhibitory synaptic modulation of a bursting pacemaker neuron. *J. Neurophysiol.*, 37:594–609.
80. Partridge, L. D. (1980): Calcium independence of slow currents underlying spike frequency adaptation. *J. Neurobiol.*, 11:613–622.
81. Partridge, L. D., and Stevens, C. F. (1976): A mechanism for spike frequency adaptation. *J. Physiol.*, 256:315–332.
82. Pinsker, H. M. (1977): *Aplysia* bursting neurons as endogenous oscillators. I Phase response curves for pulsed inhibitory synaptic input. *J. Neurophysiol.*, 40:527–543.
83. Plant, R. E. (1978): The effects of calcium on bursting neurons: A modeling study. *Biophys. J.*, 21:217–237.
84. Poggioli, J. and Putney, J. W., Jr. (1982): Net calcium fluxes in rat parotid acinar cells: Evidence for a hormone-sensitive calcium pool in or near the plasma membrane. *Pflugers Arch.*, 392:239–243.
85. Raines, A., Niner, J. M., and Pace, D. G. (1973): A comparison of the anticonvulsant, neurotoxic and lethal effects of diphenylbarbituric acid, phenobarbital and diphenylhydantoin in the mouse. *J. Pharmacol. Exp. Ther.*, 186:315–322.
86. Schwartzkroin, P. A. (1978): Secondary range rhythmic spiking in hippocampal neurons. *Brain Res.*, 149:247–250.
87. Smith, T. G., Jr., Barker, J. L., and Gainer, H. (1975): Requirements for bursting pacemaker potential activity in molluscan neurones. *Nature*, 253:450–452.
88. Stinnakre, J., and Tauc, L. (1973): Calcium influx in active *Aplysia* neurones detected by injected aequorin. *Nature New Biol.*, 242:113–115.
89. Strumwasser, F. (1973): Neural and humoral factors in the temporal organization of behavior (Seventeenth Bowditch Lecture). *Physiologist*, 16:9–42.
90. Thompson, S. H. (1977): Three pharmacologically distinct potassium channels in molluscan neurones. *J. Physiol. (Lond.)*, 265:465–488.
91. Thompson, S. H., and Smith, S. J. (1976): Depolarizing afterpotentials and burst production in molluscan pacemaker neurons. *J. Neurophysiol.*, 39:153.
92. Wilson, W. A. (1982): Patterned bursting discharge of invertebrate neurons. In: *Cellular Pacemakers*, vol. I., edited by D. Carpenter, pp. 219–235. Wiley, New York.
93. Wilson, W. A., and Wachtel, H. (1974): Negative resistance characteristic essential for the maintenance of slow oscillations in bursting neurons. *Science*, 186:932–934.
94. Wilson, W. A., and Wachtel, H. (1978): Prolonged inhibition in burst firing neurons: Synaptic inactivation of the slow regenerative inward current. *Science*, 202:772–775.
95. Winegard, S. (1982): Calcium release from cardiac sarcoplasmic reticulum. *Annu. Rev. Physiol.*, 44:451–462.
96. Yellen, G. (1982): Single Ca^{+2} activated non-selective cation channels in neuroblastoma. *Nature*, 296:357–359.
97. Zbicz, K. L., and Wilson, W. A. (1981): Barbiturate enhancement of spike frequency adaptation in *Aplysia* giant neurons. *J. Pet.*, 217:222–227.
98. Zierler, K. (1981): A critique of compartmental analysis. *Annu. Rev. Biophys. Bioeng.*, 10:531–562.